Physics – Uspekhi **66** (12) 1224 – 1247 (2023)

REVIEWS OF TOPICAL PROBLEMS

PACS numbers: **05.45. – a**, 87.19.L –, **87.85. – d**

Stochastic processes in the brain's neural network and their impact on perception and decision-making

A N Pisarchik, A E Hramov

DOI: https://doi.org/10.3367/UFNe.2022.12.039309

Contents

Abstract. The article deals with the influence of stochastic dynamics of the brain's neural ensembles on the perception and processing of sensory information, as well as on decision-making based on it. The review considers sources of noise in the nervous system during sensory information processing, as well as some nervous system strategies of compensating for or taking into account stochastic processes. Experiments and mathematical models are discussed in which stochastic brain dynamics begins to play a significant role in the perception of sensory information. Particular attention is paid to brain noise research paradigms such as the perception of weak stimuli close to the sensitivity threshold and bistable ambiguous stimuli. Methods for assessing brain noise using both psychophysical experiments and direct analysis of neuroimaging data are described. Finally, some issues in applying the concept of stochastic brain dynamics to problems in the biomedical diagnosis of various neurological diseases are considered.

A N Pisarchik [1, a], **A E Hramov** [2, 3, b]

[1] Center for Biomedical Technology, Universidad Politécnica de Madrid, Campus Montegancedo, Pozuelo de Alarcón, Madrid, 28223, Spain

[2] Immanuel Kant Baltic Federal University, ul. Aleksandra Nevskogo 14, 236041 Kaliningrad, Russian Federation

[3] Samara State Medical University, ul. Chapaevskaya 89, 443099 Samara, Russian Federation

E-mail: [a] alexander.pisarchik@ctb.upm.es, [b] aekhramov@kantiana.ru

Received 8 December 2022

Uspekhi Fizicheskikh Nauk **193** (12) 1298 – 1324 (2023)

Translated by V L Derbov

Keywords: neural networks, brain, stochastic process, perception, mathematical models, psychophysics, stochastic/coherence resonance, electroencephalogram and magnetoencephalogram analysis

One must still have chaos in oneself
to be able to give birth to a dancing star.
Friedrich Nietzsche, *Thus Spoke Zarathustra*

1. Introduction

We are surrounded by complex systems of various scales: from biomolecules and living cells to socio-economic systems and technogenic networks. As a rule, in the process of their evolution, such complex systems demonstrate the formation of dissipative structures, caused by intrinsic nonlinear and nonequilibrium interactions and stabilized by the exchange of energy, matter, and information with the environment [1–3]. Issues regarding the nonlinear dynamics of such systems, including those of a biological nature, have been brought up many times by the *Physics–Uspekhi* journal [4–11]. Along with the dynamical component, the behavior of such systems often includes certain forms of noise, which, instead of representing a negative perturbation, turn out to be a fundamental factor of the nonlinear dynamics occurrence and increase the efficiency of the system behavior or its productivity for solving a certain problem or implementing a desired protocol.

Many examples of this useful role of noise can be found in physics and biology; in particular, we can mention quantum phenomena accompanied by noise [12], stochastic [13, 14] and coherence [122] resonance, noise-enhanced stability [15], induced second-order phase transitions [16, 17], enhanced

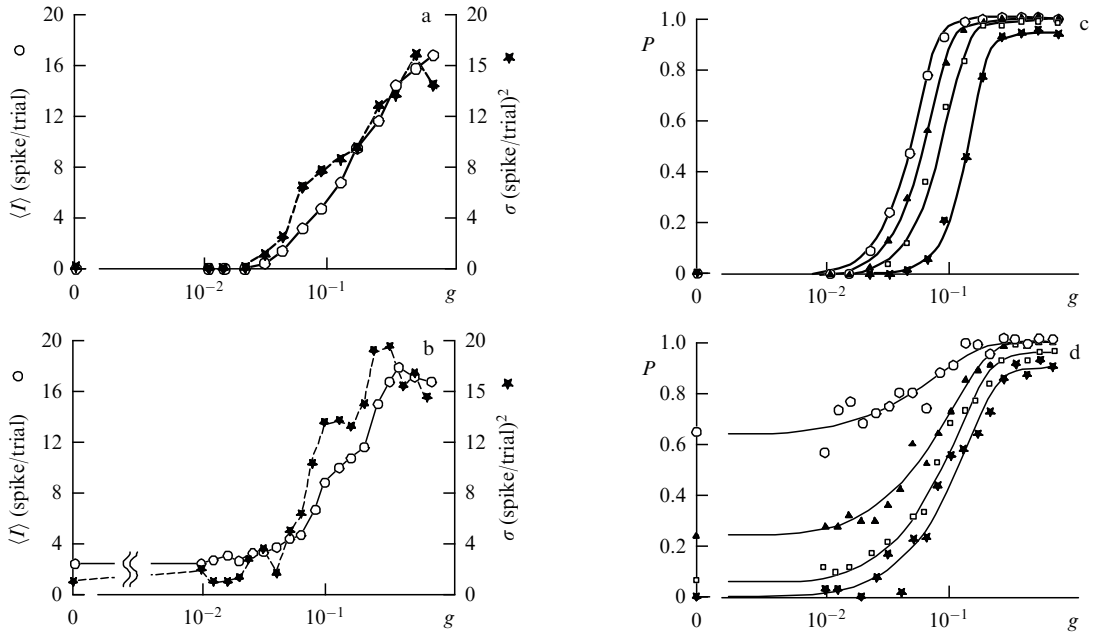

Figure 1. (a, b) Mean value $\langle I \rangle$ and variance σ of the number of spikes generated by visual cortex neurons when demonstrating one and the same visual stimulus in the form of a grid on a monitor screen, depending on image contrast g. Mean response is shown by circles (the left ordinate) and response variance by stars (right ordinate). (c, d) Probability P of observing the number of spikes I in the response to an individual stimulus presentation exceeding some threshold I_0. In Fig. c, threshold responses are $I_0 = 1$, 2, 4, and 8 spikes per stimulus (circles, triangles, squares, and stars, respectively); in Fig. d, thresholds are 5, 10, 15, and 20 spikes per stimulus (circles, triangles, squares, and stars, respectively). In all cases, the probability grew monotonically from a small value at low contrast levels to an asymptotic probability of about 1.0. Curves approximating the data correspond to the Weibull distribution integral in the following form: $P = \delta - (\delta - \gamma) \exp\left(-(m/\alpha)^{\beta}\right)$, where δ, γ, m, α, and β are positive constants whose values are chosen to provide the best approximation of experimental data. (a, c) Data on detecting the activity of a neuron from the primary visual cortex (striate cortex) of a monkey; (b, d), of a neuron from the primary visual cortex of a cat. (Adapted from Ref. [27].)

diffusion in communication networks: ordering by noise increase [18], excitation transfer by noise in light-collecting complexes of natural photosynthesis [19], information transmission in bistable and excitable systems and in quantum channels [20, 21], as well as improved productivity of neural activity, cognitive processes, or detection of information signals against a noise background [22]. At the socio-economic macrolevel, random strategies also turned out to be very successful in increasing the efficiency of many social systems in the context of game theory, control of hierarchic organizations, political institutions, and financial markets [23].

In this review, we will understand noise as a random or stochastic process that represents evolution, discrete or continuous in time, in the form of a random variable. In many fields of science we are faced with recording some experimental data that represents a more or less chaotic signal or image. Therefore, the interpretation of these observations is associated with uncertainty, which can be reflected by using probabilities to represent them. A function whose value for each value of the independent variable is a random variable is called a random function. Hence, a random function can be considered an infinite set of random quantities, depending on one of several independently changing variables. Random functions for which the independent variable is time t are usually referred to as stochastic processes. The foundations of the general theory of random processes were developed by Russian mathematicians A N Kolmogorov, A Ya Khinchin, and E E Slutsky [24–26].

Returning to living systems, we should note that one of their fundamental properties, striking even with the most superficial analysis, is their variability. Variability in the perception of information or some response to impact is observed even when external conditions, such as sensory input or the goal set for the organism, are maintained as constant as possible. This variability is observed not only at a level of the entire organism, but also at a level of individual neurons. For illustration, Fig. 1a, b shows the response characteristics of a single neuron in the primary visual cortex of a macaque and a cat, recorded invasively during repeated presentation of the same visual stimulus (grid on the monitor screen), depending on the image contrast g [27]. Circles show the mean value $\langle I \rangle$ of spikes generated by the neuron during the stimulus observation, stars show the variance σ of the number of spikes (the animals were shown about 100 stimuli (trials), using which the mean value and variance were calculated). It is clearly seen that, upon increasing the image contrast, a monotonic growth of both the mean number of spikes in the neural response and the variability of this number is observed, which is fixed by the growth of the variance of the number of spikes in the neural response. In this case, as shown in Fig. 1c, d for the same neurons, the probability P of observing the number of spikes I in the response to an individual stimulus presentation exceeding a certain threshold I_0 is described by the Weibull distribution, i.e., the impulse generation by an individual neuron in the visual cortex network has a probabilistic nature.

What can this variability be associated with? From trial to trial, it can be determined by two factors: the deterministic properties of a complex neural network and the stochastic properties, i.e., irregular random perturbations or noise which hampers and/or distorts the transmission of information in the neural ensemble. First, the initial state of the network before the stimulus presentation will be different

every time, which will lead to different neural responses and, as a consequence, different behavioristic reactions. This resembles the known phenomenon of deterministic chaos, when a Lyapunov-unstable deterministic dynamical system is characterized by an extremely strong dependence of its phase trajectory on the initial conditions [28]. Since the aspects of variability as a property of the neural ensemble itself have been multiply discussed in the literature, for example, in the most significant reviews [29–32], here we will not dwell on these issues. Second, the mechanism of noise influence on the perception and interpretation of sensory information by the brain at all hierarchic levels of the nervous system is the least studied. There are a number of review papers [22, 33–35] considering these issues; however, a lot of time has passed since their publication, and new results have been accumulated, which require systematization and further discussion. Note also that many of these papers are focused on the variability of the neural reaction or behavior; therefore, in the present paper, we focus our attention on the aspects of brain operation which can be directly associated with and/or explained by the presence of noise.

In the present review, we will dwell on the question of how the stochastic dynamics of the brain neural ensemble can affect our perception and processing of sensory information, as well as decision-making based on it. Section 2 considers the nature of noise in the nervous system when processing sensory information, as well as some strategies of the nervous system aimed at compensating for the noise of taking it into account. Section 3 considers experiments and mathematical models where the stochastic brain dynamics begins to play a role in the perception of sensory information. We pay particular attention to such paradigms of noise study as the perception of weak stimuli close to the sensitivity threshold and bistable ambiguous stimuli, because, on the one hand, the problem of detection or choosing this or that interpretation of such an object is determined exactly by random processes and, on the other hand, this approach allows creating simple and adequate mathematical models, which can be easily checked in psychophysical experiments. Here, we also briefly consider the effect of coherence and stochastic resonance in the brain neural network, capable of playing a positive role in the detection and processing of stimuli by the brain. In Section 4, we present some methods for assessing the brain noise both using psychophysical experiments and as a result of direct analysis of neuroimaging data. Finally, Section 5 discusses the issues of applying the concept of brain stochastic dynamics to problems of biomedical diagnosis of various diseases.

Note also that the problem of noise affecting the functions of the nervous system is interdisciplinary and its solution requires attracting both neurobiologists and neurophysiologists, on the one hand, and specialists in statistical physics for mathematical modeling of processes in the central nervous system, on the other hand.

2. Sources of noise in sensory information processing by the brain

We begin our review by considering the nature and mechanisms of noise generation in the central nervous system (CNS). Since the brain is intended to receive and process information and to act in response to it, in this section, we will dwell on the question of how noise appears and transforms in neural ensembles of the brain. In the subsequent sections, we will consider the noise contribution to the variability of the organism's behavior at every level of the behavioristic cycle. Figure 2 illustrates the stages of processing sensory information in the CNS, affected by external and internal stochastic impacts. First, the external noise component is initially present in signals characterizing the external stimuli independent of their type (olfactory, auditory, tactile, etc.) Second, endogenous noise sources are always present in the brain in the form of random synaptic connections and spontaneous neural activity. Finally, the integration of neurons into ensembles leads to a change in the total intensity of this noise, which can both grow and become stabilized due to the collective interaction of neurons. Let us consider these processes in more detail.

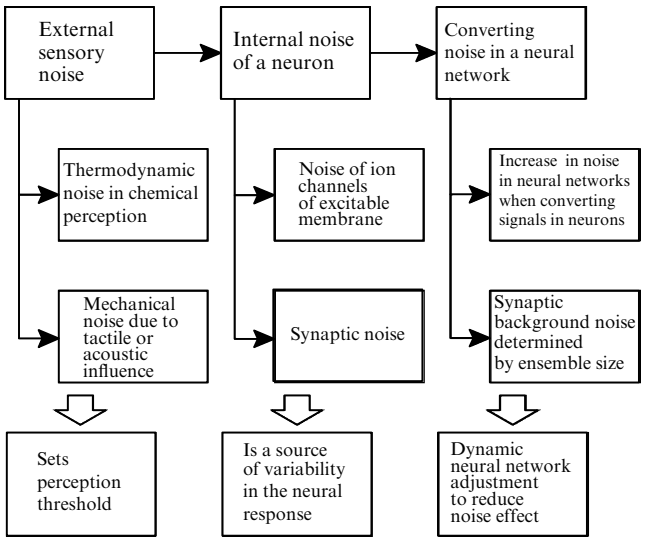

Figure 2. Main sources of noise, its transformation, and consequences of exposure in the central nervous system during the processing of sensory information.

2.1 External sensory noise

External sensory stimuli independent of their modality (visual, audial, olfactory, etc.) always carry a stochastic component, since they are either thermodynamical or quantum mechanical in nature [34]. For example, vision includes the absorption of photons that arrive at the photoreceptor with intervals obeying the Poisson process. This imposes a physical limitation on the contrast sensitivity of vision, which decreases at low levels of illumination, when fewer photons arrive at the eye photoreceptor [36]. In a similar way, all forms of chemical perception, including olfaction and gustatory sensations, are subject to the influence of thermodynamic noise, since molecules arrive at the receptor at a random rate due to diffusion. At the same time, receptor proteins are limited in their ability to count the number of signal molecules exactly [37].

At the first stage of perception, the sensory stimulus energy is converted into a chemical signal, for example, through the absorption of photons or binding of odor molecules by ligands, or into a mechanical signal, for example, by moving hair cells in the ear under the action of an acoustic wave. The subsequent process of transmission amplifies the sensory signal and transforms it into an electric one directly or indirectly via secondary cascades of sensory information transmission. Any sensory noise already present

or arising in the amplification process (random processes of transformation and amplification [38]) increases the observed variability from trial to trial of the sensory system by one stimulus. In fact, the noise level sets the perception threshold for subsequent stages of sensory information processing, since signals weaker than the noise cannot be distinguished from it after amplification. This is obvious from the information theory, following which we are to conclude that it is impossible to extract more information at further stages of processing, even free of noise, than there was at previous stages [39]. Therefore, to reduce the noise in a sensory system, living organisms often 'pay' a high energy and structural cost at the first sensory stage of information processing by, among other things, increasing the number of receptors. For example, Ref. [40] shows that the photoreceptors of a fly consume about 10% of energy at rest and the eye optics, more than 20% of the useful load in flight.

2.2 Intrinsic synaptic and electric noise in neurons

The main endogenous source of noise in the brain is the intrinsic synaptic and electric noise in neurons. If similar stimuli are presented to neurons in a series of similar trials, the response of neurons in the form of a sequence of resulting action potentials is usually characterized by a distribution of inter-spike intervals (ISIs) that varies in different trials [27, 32, 41–44]. This variability of the neuron response amounts to milliseconds or less [41, 45–49], but since the neurons of the brain cortex can detect the coincidence of action potentials in the millisecond time scale [50, 51], the above order of accuracy of synchronizing neural responses is quite capable of being physiologically significant. Indeed, it was shown that the accuracy of synchronizing the time of action potentials on a single neuron in the milli- and submillisecond scale has a behavioristic value for the processing of sensory information [52, 53] and motion control [54, 55]. To what degree the neural variability contributes to information processing or whether it yields only a stochastic component is a fundamental unresolved problem of understanding the neural encoding mechanisms [32, 34, 53, 56].

At present, it is impossible to unambiguously answer the question of whether seemingly random activity is really random. Indeed, the variability of neural activity (both during simulation and between stimuli) demonstrates statistical characteristics, such as the mean value and variance, corresponding to characteristics of random processes. However, even if the statistics of the spike activity of neurons corresponds to the statistics of a random process, it does not necessarily mean that the spikes are generated as a result of a random process. From the Shannon theory of information [57], it is known that at optimal encoding to maximize the information transmission the neural signals will appear to be random [56]. As a result, we usually observe a high level of noise in activation patterns of individual neurons, which is usually characterized by the coefficient of variation (CV) in the distribution of inter-spike intervals, also referred to as the Fano coefficient. The CV is defined as the ratio of the standard deviation to the mean value of the ISI distribution. Real neurons often demonstrate a large $\mathrm{CV} \approx 1$, which is quite expected, since the sequence of generated neural spikes is a Poisson process [58]. However, the variability of spike generation is not the same for all neurons. Some neurons of the cortex possess greater variability with $\mathrm{CV} \gtrsim 1$ [27, 59], whereas in other neurons $\mathrm{CV} \approx 0$ [60, 61]. Moreover, neurons with high and low variability are often observed in the same region of the brain, and one neuron can respond with a different degree of variability depending on the type and presentation conditions of the stimulus [32, 41–44].

The variability of neural response from stimulus to stimulus, on the one hand, is determined by changes in the intrinsic state of neurons and neural networks and, on the other hand, by random processes inside the neurons themselves and neural networks [62–64]. It still remains unclear to what degree each of these factors contributes to the total observed variability from trial to trial, especially as network effects, in spite of the noise presence, can reduce the variability, as will be shown in Section 2.3. Anyway, the effect of noise on cell functions will inevitably increase the variability of neural response; therefore, we can compare the variability caused, for example, by external noise with the total observed variability, which will give us an idea of relative noise contribution to the neural response variability.

In each neuron, the noise is determined by random processes at a cell level and can increase as a result of nonlinearity of biochemical and biophysical reactions and network interactions. Such processes include the production and degradation of proteins, opening and closing ion channels, merging of synaptic vesicles, diffusion, and binding of signal molecules with receptors [34]. It seems possible to hypothesize that the averaging of a large number of stochastic processes effectively removes the randomness of individual elements. However, this is not quite so. Neurons execute linear operations, including significant amplification of the signal and positive feedback. Therefore, even small biochemical and electrochemical fluctuations can substantially affect the reaction of the entire cell. For example, when the membrane potential approaches the excitation threshold, the generation of the action potential by the neuron becomes very sensitive to noise [65–67].

At the initial stages of studying neural mechanisms, large-size neural structures were often used as study subjects, for instance, the gigantic axon of a squid, the diameter of which can approach 1 mm). With the scale of these structures taken into account, a conclusion was made about the deterministic nature of the functioning of such structures, since they involve a large number of signal molecules, and random fluctuations are really averaged. Along with this, many neurons are very small: the cerebellum parallel fibrils have a mean diameter of 0.2 μm, the diameter of C fibers participating in the sensory and pain transmission fluctuates between 0.1 and 0.2 μm, and the nonmyelinated axon collaterals of pyramidal cells that form most local cortico-cortical connections have an average diameter of 0.3 μm. Similarly, most CNS synapses have sizes up to a micron. With such small spatial scales, the number of molecules taking part in the generation of action potentials is not large, and the influence of noise drastically grows [66], since the opening of the ion channel affects the membrane potential, which increases with a decrease in the axon diameter d proportionally to the input resistance of the membrane. In axons with $d < 0.3$ μm, the input resistance is quite large, so that the spontaneous opening of individual Na^+ channels in the neuron at rest can cause spontaneous generation of an action potential in the absence of any other inputs. Such random spikes become more frequent as d decreases, making axons with $d < 0.08-1.0$ μm useless for spike transmission. It is interesting that this 'noise' limit corresponds to the minimum diameter of axons observed in various animal species.

The spontaneous opening of individual Na^+ channels can also affect the initialization and propagation of the action potential in the axon, although this effect is rarely taken into account, and all post-synaptic variability is traditionally attributed to synapses [34]. This becomes particularly important when the axon input resistance is large enough so that a small number of ion channels can support the potential propagation [68]. Mathematical modeling [69] has shown that, in axons 0.1–0.5 μm in diameter, the noise of ion channels introduces significant fluctuations in the generated potential propagation. Hence, the greater the variability of postsynaptic responses arising due to the noise of axonal channels, the longer and thinner the presynaptic axon. Moreover, the ion channel populations can preserve the axonal activity memory for a few hundred milliseconds thanks to the complex interaction between the intrinsic states of ion channel populations and the membrane potential. This dependence on the prehistory leads to the fact that some spike patterns will be less affected by noise than others [69]. Such a 'message dependent' noise is observed, for example, in the neurons of mamillary bodies [70].

Another source of synaptic variability is 'synaptic background noise,' understood as an intense synaptic impact of thousands of synapses on neocortical cells [71, 72]. Experimental and numerical analysis of dendrite mechanisms allowing individual synapses to interact shows that such background synaptic activity includes not only the noise but also a certain deterministic structure [73–75]. Nevertheless, there are microscopic sources of real noise present in each synapse affecting the stochastic component of the synaptic background activity and the excitation of neurons [74]. First, this is the spontaneous postsynaptic current (SPC), which can be recorded in the absence of presynaptic input. The SPC is caused by random events in the mechanism of synaptic transmission, such as the spontaneous opening of the intracellular Ca^{2+} store, noise in the Ca^{2+} synaptic channel, spontaneous launching of vesicle release, or spontaneous merging of vesicles with a membrane [76, 77]. All the mentioned noise sources give rise to amplitude variability of the postsynaptic current at a level of $CV > 0.2$ [78, 79]. Second, these are failures of neurotransmitter release: when the action potential enters the presynaptic terminal, the neurotransmitter releases with a certain probability P_r [80, 81]. The release probability varies from 0.2 to 0.8 in synapses [82, 83], which gives rise to significant noise in information transmission through the neuron, associated with random neurotransmitter release.

Note several additional factors with regard to the neuron noise related to biochemical processes with a small number of molecules and therefore also subject to significant thermodynamic noises: (1) fluctuations in the number of neurotransmitter molecules released from one vesicle (about 2000), arising due to variations in the vesicle size and the concentration of the vesicular neurotransmitter [84, 85]; (2) fluctuations related to the randomness of diffusion of a relatively small number of molecules ($CV > 0.16$ [86]); (3) randomness in the sites of vesicle release, spatially distributed over the synaptic active zone ($CV > 0.37$ [86]); (4) noise in the synaptic-receptor channel increasing variability, especially if only a small number of receptors are used [87]; and (5) the number and the amount of receptor proteins in any synapse possibly changing stochastically with time, since the expression of proteins is limited by thermodynamical noise [88].

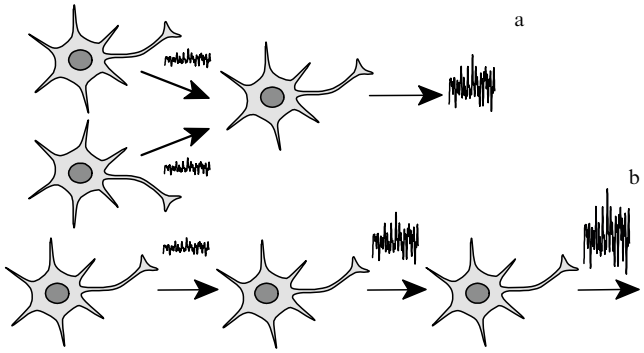

Figure 3. Schematic illustration of noise conversion in neural networks in which potential-graded neurons linearly sum inputs. (a) Summation of signals in one neuron. If the incoming signals have independent noise, then the noise level in the postsynaptic neuron will change in proportion to $\sim \sqrt{N}$, where N is the number of signals. If the noise in the signals is perfectly correlated, then the noise in the neuron will vary proportionally to $\sim N$. (b) Passage of a signal through a series of neurons. In this case, the noise level increases as $\sim \sqrt{N}$, where N is the number of consecutive neurons.

2.3 Noise in neuron ensembles

The noise in an individual neuron begins to affect other neurons when the neurons join into neuron ensembles. At the same time, it is clear that neural networks can support stable activity in the presence of noise. This property is determined by several mechanisms controlling the general level of noise in a neural network. Figure 3 illustrates various situations of noise conversion when the signals pass through simple neural networks, where the neurons with a gradient potential linearly sum up the inputs. Figure 3a illustrates the convergence of N signals at one neuron. If the input signals from presynaptic neurons have independent noise, then the level of noise in the postsynaptic neuron will change proportionally to the square root of the number of signals ($\sim \sqrt{N}$), whereas the signal changes proportionally to N. If the noise in the signals is perfectly correlated, then the noise in a neuron will also change proportionally to N. Figure 3b shows the sequential transmission of a signal through a chain of N neurons. In this case, the noise level increases proportionally to the square root ($\sim \sqrt{N}$) of the number of sequentially connected neurons, i.e., repetition in the network leads to the growth of the correlated noise. This allows an important conclusion that the involvement of a large-size neural ensemble in brain information processing must lead to an increase in the noise level, which will be recorded in such an ensemble.

At the same time, it is intuitively clear and confirmed experimentally that noise processes are controlled by the neural network at the expense of its connection topology and neuron types. Apparently, a highly parallel and distributed but compact CNS structure helps to limit the amount of accumulated noise in the brain network. Indeed, in contrast to the sequential transmission of signals, as shown in Fig. 3b, the parallel connections in the neural ensemble will not increase the noise due to network interactions. Other computational operations executed by each neuron can also change the character of noise increase in a neural network. The linear operation of amplification retains the signal-to-noise ratio unchanged. Nonlinear operations, such as multiplication or threshold filtering, affect the noise increase in different ways. Generally, multiplication operations increase

the output signal CV, whereas threshold filtering decreases the CV. Since the noise propagation and action in ensembles of neuron-like nonlinear elements have been considered in a number of papers [89–92], we will not dwell on this issue here.

It is quite probable that noise control in the CNS can also be realized at a level of individual synapses. For example, experimental data testify that the mean level of neural activity is supported by mechanisms of homeostatic plasticity, which dynamically set the synaptic strength [93], expression of ion channels [94], or release of neuromodulators [48]. In turn, this implies that the neural networks can dynamically regulate their connections to attenuate/amplify noise effects. One of the possible mechanisms of such regulation is considered in Ref. [72].

As was discussed in Section 2.2, a decrease in the probability P_r of neurotransmitter release reduces the information transmission to the postsynaptic cell. However, by increasing the conductivity with the decrease in P_r in such a way that the product of the conductivity and P_r remains constant, it is possible to retain the efficiency of spike transmission in the neural network. In this case, the mean value is independent of the release probability, and the variance increases as $(1 - P_r)/P_r$. Hence, the variance grows with decreasing P_r. Therefore, both breakdowns in neurotransmitter release and the variability of conductivity can be useful for information transmission.

Figure 4 illustrates the fact that the noise in the synapses can play a constructive role in information transmission in the case of weak input signals. Figure 4a shows that reliable synapses ($P_r = 1$) with constant conductivity are 100% efficient, but only when the total input is above the spike generation threshold (compare the left and right images). For comparison, unreliable synapses ($P_r < 1$) with the conductivity scaled to save the transmitter expenditures (as was described above) can transmit more information when the signal is below the threshold, but in this case the efficiency of information transmission is worse than when the signal is above the threshold (Fig. 4b). Hence, reliable synapses with variable conductivity behave like unreliable synapses with constant conductivity (Fig. 4c). From the performed analysis, it becomes clear that the noise increases the information transmission efficiency if the threshold is too high and decreases if it is low. The optimal strategy implies maximum reduction of noise followed by setting the spike generation threshold to maximize the information transmission. A simultaneous increase in the release probability and decrease in the conduction variability reduce the noise. In addition, the nervous system has one more option: to increase the neural network complexity by adding extra synaptic connections, i.e., to allow some axons to establish several synaptic connections on the postsynaptic cell [95]. This averages out the noise and, therefore, partially compensates for the unreliability of synapses [96, 97]. This is exactly the strategy 'followed' by reliable synapses, such as the neuromuscular junction or the calyx of Held, which are furnished with multiple unreliable sites of neurotransmitter release [98].

It was also shown that in some neurons input signal doubling leads to an increase in the output signal by less than two times [99, 100]. This means that the presynaptic and intracellular noise weaken as the signal passes through such a neuron. The relatively weak brain noise testifies to the fact that the CNS neuron networks are organized to prevent local noise accumulation with the propagation of neural signals [101].

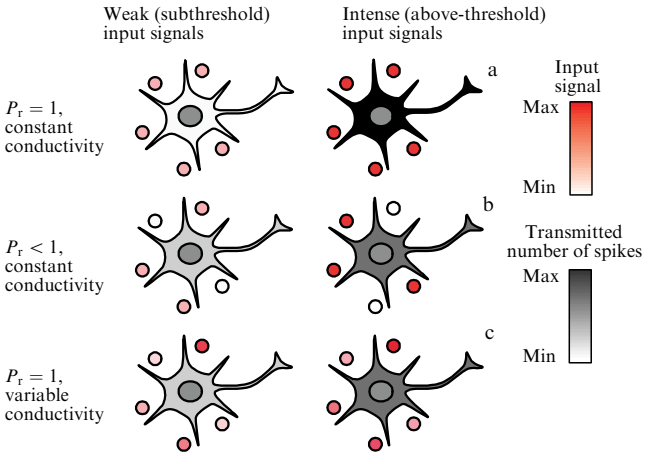

Figure 4. Illustration of the constructive role of synaptic noise in information transmission in the case of weak input signals. Here, synaptic inputs are shown as circles; the intensity of the red color reflects the intensity of their activity. The number of neuron spikes is indicated from white to black, with a higher spike probability (black) corresponding to a higher information transmission rate. (a) Reliable synapses ($P_r = 1$) and no variability in postsynaptic conductance. If the threshold is too high, there are no spikes (left), but if the threshold is lowered a little, spike transmission becomes 100% reliable (right). (b) Unreliable synapses ($P_r < 1$) and no variability in postsynaptic conductance, with conductance proportional to $1/P_r$ (to maintain transmission efficiency). In this case, a postsynaptic spike is possible when the input signal is weak, thus transmitting some information (left). However, when the input signal is strong, unreliable synapses lose information (right; compare with (a)). (c) Reliable synapses ($P_r = 1$) but with variability in postsynaptic conductance. Information transfer occurs in approximately the same way as in unreliable synapses with constant postsynaptic conductance (compare with (b)). (Adapted from [72].)

3. Role of noise in sensory information perception: experiments and models

3.1 Detection of sensory stimuli

The detection of sensory stimuli belongs to the simplest kinds of perceptive experience and is the first stage of any further processing of sensory information and decision-making. The fundamental problem that arises when solving problems of detecting sensory stimuli is that the repeated presentation of a near-threshold stimulus can unpredictably lead either to failure or to success in stimulus detection. What affects these changing perceptual judgements? To answer this question, an experiment was carried out [102, 103], in which monkeys were taught to execute a behavioristic task of detecting a stimulus. The trained monkeys communicated the presence or absence of a mechanical vibration applied to the finger tips by pushing one of two buttons. The authors focused on the analysis of neural correlates (the regions of the primary somatosensory cortex (S1) and medial-premotor cortex (MPC), shown in Fig. 5a). It was found that the activity of MPC neurons was weakly modulated by the stimulus amplitude, but correlated well with the monkeys' responses (stimulus detected — true positive (TP) or stimulus not recognized — false negative (FN)), as illustrated by Fig. 5b. On the contrary, S1 neurons did not correlate with perceptual reports from the animals, but the frequency of their excitation demonstrated a monotonically growing dependence on the stimulus amplitude (Fig. 5c). The fact that the MPC neurons correlate with behavioristic indicators, with a high frequency of spike

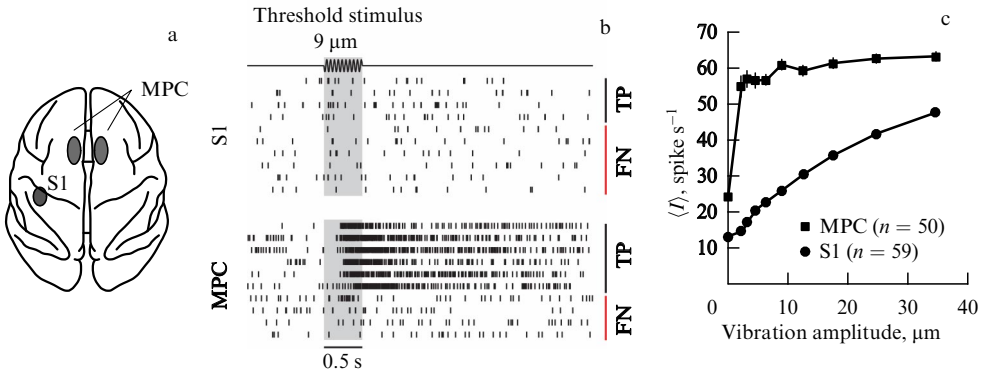

Figure 5. (a) Areas of the primary somatosensory cortex (S1) and medial premotor cortex (MPC) of the monkey brain that are neural correlates in the task of vibrotactile stimulus recognition. (b) Activity of S1 and MPC neurons during the task of detecting a stimulus with a vibration amplitude close to the threshold (9 μm), corresponding to perceptual bistability: TP — stimulus detection, FN — lack of detection at the same stimulation amplitude. (c) Average number of spikes generated by neurons in areas S1 (averaged over $n = 59$ neurons) and MPC ($n = 50$). (Adapted from [102].)

generation if the reply is 'yes' and low frequency of spikes if the reply is 'no,' from the point of view of the theory of dynamic systems indicates that the neural ensemble demonstrates bistable dynamics [104]. For the same stimulus, two possible behavioristic reactions were observed, namely, 'stimulus detection' (the 'yes' response) and 'no stimulus detection' (the 'no' response). These two reactions are related to two possible stable states (attractors) in the neurodynamic system, which coexist in one and the same state of the stimulus (i.e., the system is bistable). In this case, the presence of noise fluctuations can spontaneously transit the system from one stable state (by default, the absence of stimulus detection) to the other stable state of stimulus detection, corresponding to spike activity generation by MPC neurons (Fig. 5b). In this case, the formation of perception near the threshold is understood as a fluctuation-probabilistic transition to one of two possible bistable decision-making states, i.e., perception is the result of a cognitive decision-making process. Such understanding fits the concept proposed by Green and Swets in 1966 [105] called 'the theory of signal detection,' which is characterized by introducing a decision-making component into the sensory process structure.

The simplest mathematical model reflecting the processes involved in perception and consistent with the above neurophysiological data has been proposed in Ref. [106]. A neural area in the MPC is modeled by a network of interacting neurons organized in a discrete set of the coupled excitatory (E) and inhibitory (R) populations (Fig. 6a). The subnetwork of excitatory 'selective' neurons (EL) is connected to the sensory input λ determined by S1 neurons, reflecting the vibrotactile stimulation. All other excitatory neurons are joined into a 'nonselective' (EN) population. The network also incorporates an additional neural population that unites the inhibitory neurons (R) that regulate the general activity by implementing competition in the network. The neurons in the networks are connected by three types of receptors, which determine the synaptic currents flowing through them: AMPA, NMDA glutamate, and GABA. Neurons within an excitatory population are interconnected with high coupling strength ω^+, while those between two different selective populations exhibit uncorrelated activity, resulting in weaker connections ω^-.

The processes related to stimulus detection are understood as a probabilistic transition to one of the possible bistable decision-making states, determined by random

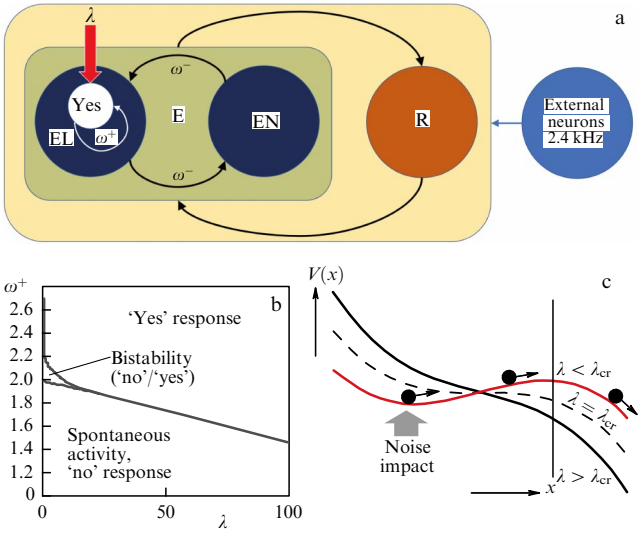

Figure 6. Model of neural populations selective for applied vibrotactile stimulation. Response 'no' is given when the selective population shows low spontaneous activity, and response 'yes' in the case of high activity. (b) Map of stationary state regimes of the model, where the most interesting region of the bistable dynamics of a selective neuron population in the context of consideration is highlighted. (c) Potential profiles of an analytically reduced one-dimensional nonlinear diffusion equation for the dynamics of neurons making a perceptual decision near the bifurcation current λ_{cr}. For small values of stimulus intensity $\lambda < \lambda_{cr}$, the potential profile is characterized by a potential well with low activity on the left and a potential barrier on the right. Perceptual decision in this case corresponds to the system leaving the well under the influence of noise by 'jumping' over the right barrier (shown by arrows). Vertical line corresponds to the boundary of the diffusion process determined by the mathematical model. As the value of $\lambda > \lambda_{cr}$ increases, the potential well and barrier disappear, which leads to an increase in the performance of making a perceptual decision.

fluctuations. In the model, the activation of a chosen excitatory population corresponds to the detection of external vibrotactile stimulation. The strength λ of the input signal arriving at this excitatory population is proportional to the strength of the presented vibrotactile stimulus (as, e.g., is encoded in S1, i.e., the input to MPC is transmitted from S1). When the stimulus is presented, there is only one population sensitive to it. To model this characteristic, a network is used consisting of two selective populations, but only one of them

is selective to the presented stimuli. In fact, in the described model, the neurons of the second selective population behave like nonselective neurons. Hence, the corresponding bistability in the considered model is specified by the state in which the excitatory populations are weakly activated (which corresponds to the absence of stimulus identification, i.e., the 'no' response) and the state when the excitatory population sensitive to the presented vibrotactile stimulus is activated strongly (which corresponds to stimulus identification, i.e., the 'yes' response).

To analyze the dynamics of this model and to find the corresponding stable states for the model of bistable perception, it is necessary to choose the parameters which determine two bistable steady states associated with low or high activity for the selective population, corresponding to the reaction of detecting 'no' or 'yes.' In Ref. [107], bistable steady states were found using the mean field approximation. The authors of Ref. [107] scanned the parameter space specified by the self-exciting weight ω^+ depending on the external action λ. Figure 6b shows the parameter space for generating the 'yes' response divided into three regions. When the weight ω^+ was high, the model generated the 'yes' response in a wide range of parameter λ values. When ω^+ was small, the selective population preserved spontaneous activity (the 'no' response) at different values of λ. Also observed was a small bistable region in the parameter space, where the selective population with some probability was either in the 'yes' state or in the 'no' state, i.e., in this region both states were stable. The bistability regime is necessary to have (for a particular external action λ) two possible responses, each of them corresponding to two possible stable states of the neural network. Together with the noise, this ensures the probabilistic behavior of the neural system of stimulus recognition and its subsequent interpretation.

The solution obtained at the level of the mean field is valid only for a stable state of the network. In Ref. [108], the authors, using an integrate-and-fire neural network, repeated the above results *in silico*. It was shown that the model dynamics agrees well with the experimental results of Lafuente and Romo [102, 103] described above. The probability of a 'yes' response increases with the growth of the sensory signal (λ), which simulates the behavior of the monkeys' neurons of the S1 region upon detection of a vibrotactile stimulus. Simultaneously, the activity of neurons taking part in the stimulus interpretation (MPC neurons) remained approximately constant at different values of the input signal λ (compare with Fig. 5b).

To emphasize more explicitly the functional role of the noise in this system, we can establish a direct connection between the variability of neurons and probabilistic behavior. It is known that the dynamics of bistable models can be reduced to a one-dimensional diffusion equation, commonly used to describe the behavioristic level in psychophysics [104, 109]. Diffusion models imply that all the information that controls the process of making a perceptive decision is continuously integrated in time until the boundary of decision-making is achieved. Taking into account the success of diffusion models in the explanation of behavioristic data, it seems probable that the decision-making processes in the nervous system are really drawn from such an accumulation of information. Diffusion models may build a bridge between neural and behavioristic models of making perceptive decisions.

The dynamics of the above bistable neural model is determined by the normal form of a saddle-node bifurcation $\dot{x} = -(\lambda - \lambda_{cr}) - ax^2$, $a > 0$, which was derived analytically from the initial equations of neural dynamics in Ref. [110]. From this description, it follows that the dynamics near the bifurcation point λ_{cr} (between the bistable and the only stable steady states) is slow and limited by the central manifold. The initial dynamics of the population neurons corresponds to the reduced one-dimensional diffusion equation describing the motion of a particle under the action of noise in the potential field $V(x) = -(\lambda - \lambda_{cr})x - ax^3/3$. Figure 6c shows this potential profile for different values of λ in the vicinity of the critical point λ_{cr}. The probability of perceptive detection (in the considered case of vibrotactile impact) can be considered to be the probability of leaving the lower branch of this profile under the action of fluctuations during some time after the stimulus presentation. The boundary is naturally specified by the top of the potential barrier located on the right. Note that this potential is not bistable, it only locally describes at the bifurcation point the dynamics of the exit from the state of spontaneous dynamics of the neural ensemble, which is sufficient to solve the problem of stimulus detection. A more complex bistable model with a double-minimum potential profile will be considered below in Section 4.1 in application to the problem of recognition of ambiguous visual stimuli.

3.2 Using noise-induced resonances to improve sensory abilities

The coherence (or ordering) of neural impulses plays the key role in the efficiency of processing the information received by the brain. Multiple data on measuring the brain's electric activity indicate the presence of a sufficiently strong stochastic component or $1/f$ noise in the power spectrum [111, 112]. Nevertheless, under certain conditions, the ordering of neural activity and increase in the signal-to-noise ratio are observed, the latter ratio often demonstrating resonance behavior with respect to the noise intensity. Ordering mechanisms in neural networks have long been of interest to scientists. Such a behavior, called coherence resonance, has been discovered in a stochastic system, whose regularity reaches a maximum at a certain intensity of random perturbations [113]. Here, it should be noted that the so-called stochastic resonance [114] is a particular case of coherence resonance in the presence of an external periodic signal.

The coherence resonance is known [115] to occur in an oscillatory system near the excitation threshold. When the intensity of the applied stimulus is less than the perception threshold, the brain noise becomes amplified to overcome the threshold and cause neural activation. Keeping in mind that every neuron and every synapse contribute to the stochastic component of the neural network dynamics, to increase the noise, it is necessary to involve more of the brain's neural network [116]. Coherence resonance has been thoroughly investigated in many systems, including neural network models, such as the Rulkov map [117], FitzHugh–Nagumo [118], Morris–Lecar [119], and Hodgkin–Huxley [116] models; it was also experimentally found in distributed cortex neural networks upon processing sensory information [116]. On the other hand, the opposite resonance behavior has also been observed, called anticoherence resonance, in which the system's regularity is minimized with respect to the noise intensity [120].

In 1997, *Physical Review Letters* published an article [121] reporting the discovery of stochastic resonance in visual perception. The essence of the study was the statement that near the visual information reception threshold neural noise is tuned to maximize the signal-to-noise ratio. From the authors' conclusion, it is not quite clear how the obtained results are related to stochastic resonance, since the signal (visual stimulus) arriving at the brain was steady-state rather than periodical. Therefore, this most likely means the classical effect of coherence resonance.

To assess quantitatively the coherence resonance in neural ensembles *in vivo*, various indicators can be used [122]. Currently, the following quantities are most frequently applied: (1) normalized autocorrelation function; (2) correlation time; (3) normalized standard deviation of the peak amplitude (amplitude coherence); (4) normalized standard deviation of inter-spike intervals (time coherence); (5) probability distribution of inter-spike and inter-train intervals; (6) dominant spectral component (spectral coherence); (7) signal-to-noise ratio determined from the power spectrum; (8) semblance function; (9) entropy; (10) connectivity in the neural network (topological coherence). We do not rule out other measures of stochastic resonance in the future. A maximum in the dependence of one of the listed quantities on the noise intensity testifies to the presence of coherence resonance, and a minimum, to the presence of an anticoherence resonance.

Recently, we found coherence resonance in the distributed cortical network of the human brain by processing sensorial information using an electroencephalography (EEG) [116]. Images of Mona Lisa with various levels of contrast $I \in [0, 1]$ were presented to the tested subjects with the simultaneous recording of EEGs. The contrast was interpreted as the noise level. Then, the correlation time of EEG signals was determined. The greater correlation time corresponds to the greater coherence of the corresponding neural population. Hence, the global coherence of the neural network can be defined as the number of EEG channels demonstrating the maximum correlation time at the given image contrast.

In all participants, local coherence maxima were observed in the weak contrast zone, which corresponded to neural coherence caused by weak perception of Mona Lisa's silhouette. Another resonance was recorded in the zone of enhanced contrast, where the local maxima in different participants were distributed in a wide range of contrast levels. When the contrast increased, the additional amount of visual information caused a sharp coherence resonance of the global network. The positions of the local maxima were determined by the inherent brain noises peculiar to each subject. In this case, a coherent behavior of the frontal and occipito-parietal parts of the brain was observed.

Analysis of the electric activity of the neural network allowed reconstructing the connection between the individual brain regions in the alpha and beta frequency ranges. A resonance character of the neural network functional structure with respect to noise was discovered. The increase in the number of connections and their strength confirm that the efficient neural connection in the frontoparietal cortical network is achieved due to coherence resonance. As was shown by recent experiments with magnetoencephalography (MEG) [123], the cerebral noise in most cases helps process the sensory information with more efficiency. In particular, the level of brain noise is determined by the size of the active neural network and can change as a result of cognitive load and in the process of training to solve a particular cognitive problem. Therefore, the increased brain noise can indicate higher efficiency of information processing and improvement in cognitive functions. This discovery removes the gap between the neural noise paradigm and the theory of global working space.

In spite of considerable progress in the study of coherence in brain neural networks, e.g., the formation of neural connections via coherence resonance, some measures of coherence need further investigation, in particular, network entropy and structural coherence resonance.

Since noise affects perception, a natural question arises as to whether it is possible or not to control perception by external sensory noise. To answer this question, Mexican researchers carried out an experiment on optogenetic noise photostimulation (ONP) of transgenic mice [124]. An electrode was inserted into the stem cerebral cortex of a mouse in the region responsible for stimulation of whiskers. The mechanical stimulation consisted of pulsed pulling of the entire bundle of whiskers with a frequency of 2 Hz. Simultaneously, the neurons of the stem cortex were stimulated with blue light (470 nm) delivered from an optogenetic light-emitting diode system through an optical fiber and modulated by a noise generator. The multiunit activity (MUA) response was recorded. It was shown that the additional ONP amplifies the amplitude of neural multiunit activity and, thus, improves somatosensory perception.

To assess the coherence of MUA quantitatively, the signal-to-noise ratio was calculated. For this purpose, first, the absolute values MUA_0 were measured in the absence of whisker stimulation and then at various levels of ONP. Then, the signal-to-noise ratio was calculated for each ONP level using the formula

$$\mathrm{SNR} = \frac{\mathrm{MUA} + \mathrm{ONP}}{\mathrm{MUA}_0} \,. \tag{1}$$

The dependence of SNR on the ONP noise level was measured, demonstrating a maximum at a certain level of noise, which is evidence of a stochastic resonance.

Hence, the results presented above confirm that the noise generated by the brain can improve sensory capabilities.

In addition to animal studies, experiments on the control of perception using transcranial noise stimulation have been carried out on humans. For example, Van der Groen et al. [125, 126] showed that under certain circumstances the efficiency of image recognition can be improved by transcranial random noise stimulation (tRNS) of the brain cortex. In particular, they have found a resonance effect in decision-making at a perceptive level.

We can hypothesize that a coherence resonance in the brain response to incoming stimuli arises because of the fact that the addition of the optimal level of noise to the subthreshold signal pushes the silent neurons beyond the threshold of impulse generation. Above, we have shown the existence of a coherence resonance when adding noise directly to a sensory stimulus. However, in such cases, the external noise can merely enhance the sensitivity of peripheral receptors [127], which gives us no idea of whether the processes in the central nervous system affect the mechanism of resonance behavior in response to an increase in the noise intensity in the course of decision-making.

In the experiments by Van der Groen et al., the random-dot-motion (RDM) paradigm was used, which is frequently

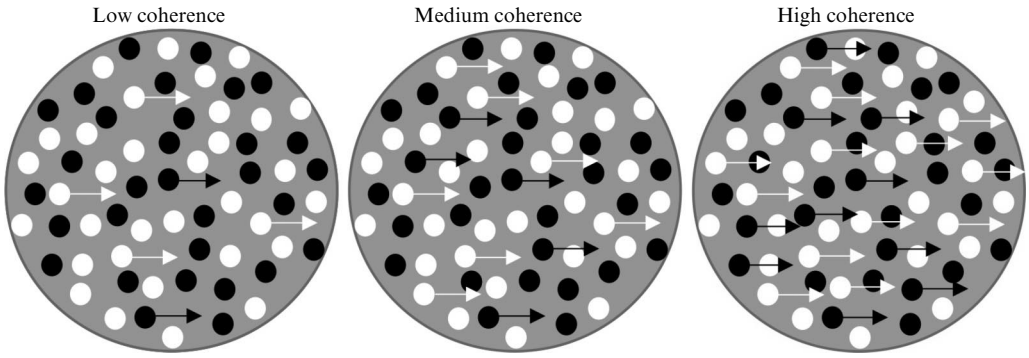

Figure 7. Illustration of the random-dot-motion (RDM) paradigm, in which participants judged which way, left or right, most of the dots were moving (shown by arrows). Difficulty of the task was determined by proportion of the number of synchronously moving points in relation to all points moving in random directions. Figure shows coherent movement of points to the right for illustration purposes, although in the experiment the points moved left and right with equal probability.

exploited in studies of perceptive decision-making and has well-characterized neural correlates [128, 129]. The RDM paradigm included the double-alternative problem of distinguishing the motion of random dots with forced choice, in which the participants had to assess the direction (to the left or to the right) of a synchronously moving point as fast and accurately as possible (Fig. 7).

Half the dots were black, half were white, and all were shown against a gray background. In the first frame, the points were arranged in a random way within a circle aperture and then moved with a velocity of 1.5 deg s^{-1} to the left and to the right. As soon as a point moved beyond the circle, it appeared at the opposite side of the aperture. The display with moving points remained visible until a response from the participant about the direction of the points' movement; the maximal duration of waiting for a response was 3 s. The participants made their choice by pressing either the left or right 'shift' key on a standard keyboard with the forefinger on the left or right hand, respectively. If the subjects did not react within 3 s, the motion stimulus was quenched, and the attempt was considered incorrect and excluded from further analysis. Instantaneous feedback was also implemented via acoustic signals of various tones. A low tone informed the subject of a correct response, a high tone an incorrect response, and a long low tone a tardy response (> 3 s). A new attempt began 2 s after the previous response.

The method of continuous stimulation was used to determine the global sensitivity to the motion of points. Namely, a part of points continuously synchronously moved to the left and to the right, while other points moved in random directions. For example, a coherence level of 3% indicates a map in which 3% of the points move coherently (to the left or to the right, depending on the trial) and the remaining 97% of the points move in random directions.

The aim of the experiment was to determine the influence of transcranial random noise stimulation (tRNS) on the correctness of visual recognition of the direction of coherent motion of points (to the left or to the right). To this end, a series of experiments was carried out, in which a tRNS of various intensities (0.25 mA, 0.375 mA, 0.5 mA, and 0.75 mA) was delivered to the participants. The first and the last blocks of the experiments were carried out without tRNS.

The group correct choice index (%CCI) was calculated for each level of coherence and each tRNS intensity by dividing the percent of correct responses about the direction of motion by the percent of correct responses when no tRHS was used (the base level) by the following formula:

$$\%\mathrm{CCI} = \frac{\%\mathrm{Corr}(i)}{\%\mathrm{Corr}(\text{zero noise})},$$

where i denotes each of the four tested noise intensities. It was found that the RDM estimate is affected by the noise magnitude, i.e., the tRNS intensity upon bilateral stimulation of the visual cortex (Fig. 8), whereas the unilateral stimulation (of the left or right cortex) had practically no effect on the experiment results.

From the plot, it is seen that the tRHS intensity of 0.25 mA significantly improves the characteristics of motion recognition compared to the initial level. This proves that perceptive decision-making for sensory stimuli slightly below the

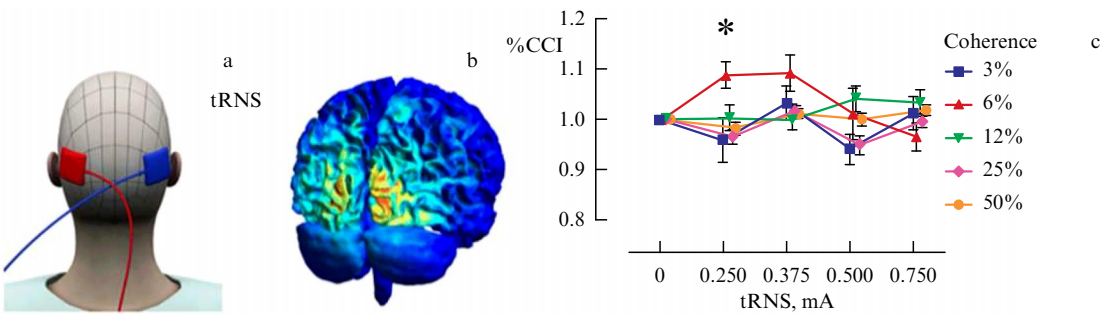

Figure 8. Bilateral transcranial random noise stimulation (tRNS) of the visual cortex. (a) Installation of electrode pads. (b) Simulated electric field strength (normE). (c) Coherence resonance in perceptual decision-making in the dot motion recognition task as a function of tRNS intensity. $^{*}p_{\text{corrected}} < 0.05$. (Based on data from [126].)

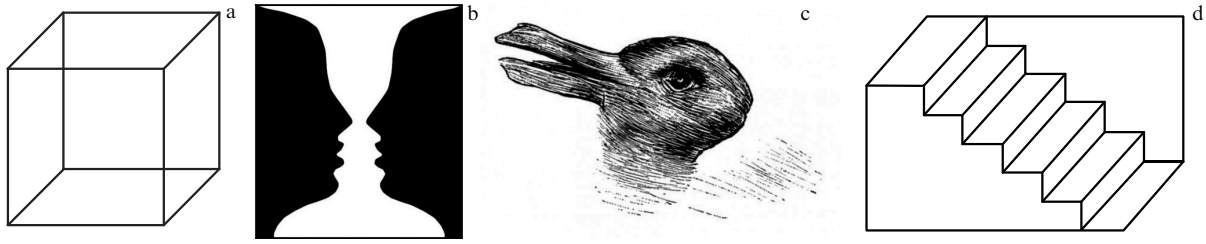

Figure 9. Examples of classical optical illusions (bistable images): (a) Necker cube, (b) Rubin vase, (c) 'duck/rabbit' illusion. (d) Schroeder stairs.

threshold can be improved by adding a small amount of neural noise to the bilateral visual cortex, which agrees with the results of other studies discussed in the present review. The obtained results can be used to improve perceptive decision-making in people with congenital or acquired neurological disorders, among aged people, or among professional athletes.

3.3 Bistable perception and interpretation of optical illusions: effect of stochastic dynamics of the brain neural ensemble

Bistable perception characterizes oscillations of perception that can be caused by certain visually ambiguous images, such as a Necker cube or Rubin vase, shown in Fig. 9. When this image is looked at for a long time, two perceptions spontaneously alternate, changing each few seconds. Such an alternation of interpretations of an ambiguous visual stimulus is explained by neural adaptation [130, 131]. Random switching between two perceptions is confirmed by multiple neurophysiological experiments in which electric or magnetic brain activity was measured [132]. At present, it is generally accepted that the biological nature of such switching is determined by the noise inherent in the brain; however, the microscopic mechanism of such fluctuations of perception remains unknown [133]. Nevertheless, there is a possibility of constructing mathematical models describing the macroscopic dynamics of such perception switchings induced by the intrinsic brain noise based on psychophysical experiments. For example, in the case of perception of ambiguous visual stimuli, the neural ensemble representing each feature can intrinsically compete for the exhibiting of the excitation degree of the subgroup of features in general. This means that one and the same ambiguous visual image can excite or inhibit different sets of neurons depending on its interpretation. In terms of mathematics, it follows that different interpretations can be due to coexisting attractors (multistability), and the brain noise leads to switching between them. Such models are referred to as attractor models [104].

Another approach to modeling bistable perception is based on neural adaptation [130, 131], since the time of subject fixation on a definite perception is nearly the same for any subject [134]. These so-called oscillatory models imply that the perceptive states are unstable, and the neural network switches between them [104]. While in oscillatory models the switching occurs even without noise mainly because of adaptation, in attractor models, the noise is the only cause of switching between coexisting attractors. In both types of models, the brain noise is of key importance for understanding the mechanisms of random switching between perceptive states.

Let us consider the attractor model, in which two different perceptions of a bistable stimulus, such as the Necker cube, are associated with two stable steady states (attractors). A change in the control parameter (e.g., the contrast of the cube's faces) leads to a deformation on their basins of attraction and, finally, to a change in their stability occurring at a critical point. Such a situation may be described by a stochastic differential equation with a third-order nonlinearity,

$$\dot{x} = -4x(x^2 - 1) - 2c_{\mathrm{L}}(x - 1) - 2c_{\mathrm{R}}(x + 1) + \alpha\xi(t)\,, \quad (2)$$

which has two stable points, i.e., this model describes the dynamics of a particle in a double-well potential profile. This model is based on the assumption that each of the two neural populations (say, L and R) represents different interpretations (c_{L} and c_{R}) of one and the same ambiguous stimulus [135]. Here, x is the state variable proportional to the difference between neural activities of two competing neural populations, and $\xi(t)$ is Gaussian white noise with a zero mean value and intensity α. Equation (2) is derived from the energy function $\mathrm{d}E/\mathrm{d}x = -\tau\dot{x}$ describing the alternation of bistable image perception in terms of the activation of neural populations.

In the case of a Necker cube with $\tau = 1$, two states, c_{L} and c_{R}, correspond to two interpretations of the cube orientation [136]. If the contrasts of two sets of faces *1–2–3* and *4–5–6* (see the inset in Fig. 10a) change simultaneously in opposite directions (while one increases the other decreases), then it is possible to use only one control parameter $c = c_{\mathrm{L}} = -c_{\mathrm{R}}$, which simplifies model (2):

$$\dot{x} = -4x(x^2 - 1) + 4c + \alpha\xi(t)\,. \quad (3)$$

The dynamics of model (3) without noise ($\alpha = 0$) approaches one of the stable states and stays there forever. If the control parameter linearly changes as $c = c_0 \pm vt$ with the rate v, the system passes through two critical points c_{f} and c_{b} back and forth, as seen from the bifurcation diagram in Fig. 10. The state of the system depends on both the initial condition c_0 and the direction of the parameter change. The change in the control parameter c leads to the deformation of the energy potential and, therefore, the volumes of attraction basins. At certain values of the parameter c, bistability occurs, which can be characterized by the hysteresis $h = c_{\mathrm{f}} - c_{\mathrm{b}}$. Because of critical deceleration, the position of the bifurcation points also depends on the rate v, i.e., h becomes greater upon an increase in v. On the other hand, the hysteresis decreases and even vanishes in the presence of noise, as shown in Fig. 10b. It is seen that, for strong noise in the model system, the hysteresis becomes negative ($h < 0$), i.e., instead of hysteresis, we are dealing with noise-induced intermittency between two metastable states.

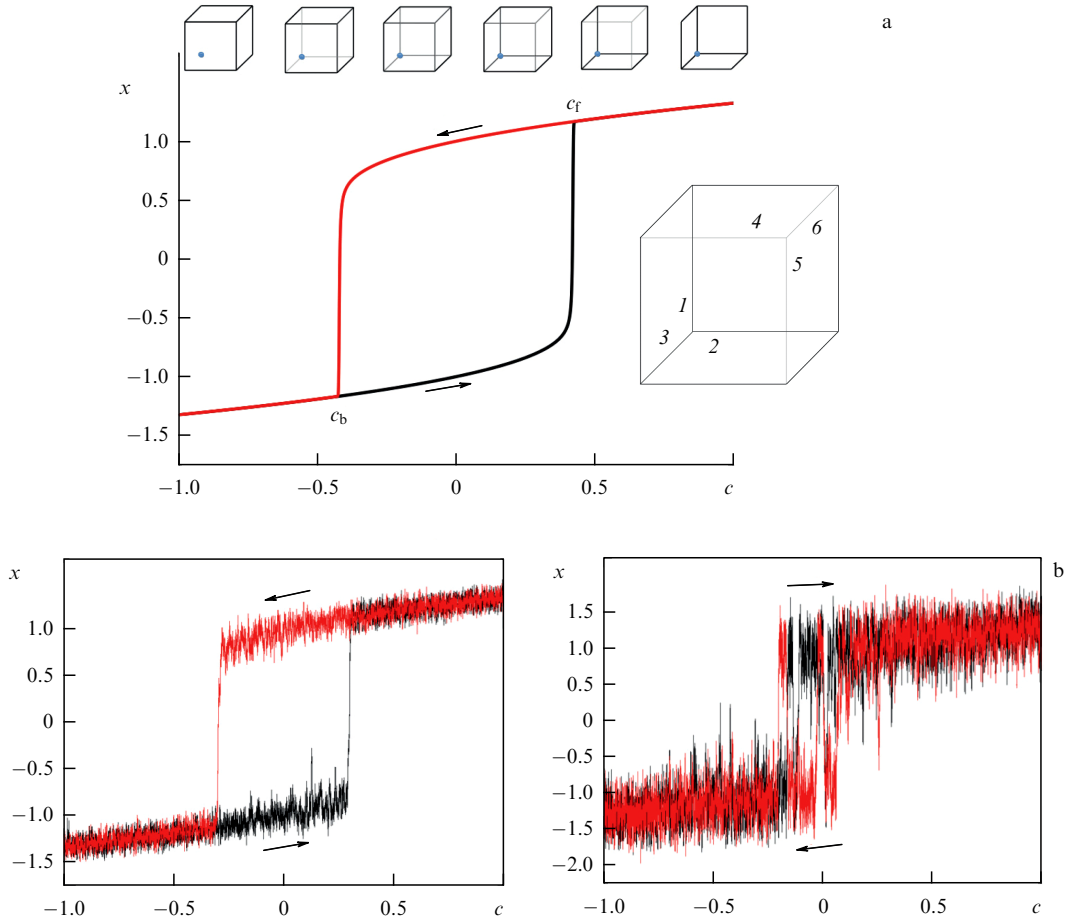

Figure 10. Bifurcation diagram of the deterministic attractor model (3) ($\alpha = 0$), showing the hysteresis of control parameter c with speed $v = 1$. Arrows indicate directions of change in the control parameter, and c_f and c_b are bifurcations of forward and reverse saddle nodes, respectively. Images of a Necker cube with different intensities of faces *1*–*2*–*3* and *4*–*5*–*6*, as shown in the inset, with a smooth transition from a left-oriented to a right-oriented cube. (b) Bifurcation diagram of model (3), demonstrating the change in the hysteresis value with increasing noise intensity from (left) $\alpha = 18$ to (right) $\alpha = 60$ at fixed speed $v = 1$.

Based on the attractor model (3), the following psychological experiment was carried out in Ref. [136]. A Necker cube with a changeable contrast of faces was displayed on a computer monitor before the subject. The contrast changed in two directions (first increased and then decreased at rate v). The subjects had to push the key on the computer keyboard only once at those moments when they distinguished the first change of the cube orientation from left hand to right hand and in the back direction. The difference between the times of pushing the keys in two directions was considered the hysteresis, which depended on both the rate of the contrast change and the brain noise. Since the rate was similar for all subjects, the difference in hysteresis was due only to the difference in brain noise, which can be applied to relative estimates and comparing the noise in different subjects.

Experimental results confirmed the numerical results obtained by means of the energy model. In particular, the experimental confirmation of negative hysteresis allowed us to conclude that the brain noise is so strong that perception bistability does not exist. In a real situation, instead of bistability, we are dealing with switchings between two metastable perceptive states.

An alternative approach to the modeling of bistable perception and the influence of brain noise on it is based on the interaction and competition of representative populations of neurons [137–139]. Such so-called oscillatory models have been proposed to describe a random process of training in which the competition between perceptive populations of neurons occurs via mutual inhibition accompanied by a slow adaptation of the dominant population. Notably, the authors of Ref. [140] hypothesize that adaptation plays a key role in making the perceptive choice, and the brain noise ensures the randomness in switching between different interpretations (excitation of perceptive neuron populations) [141].

Let us consider the synergetic Haken model [142], which consists of two coupled subsystems,

$$\dot{x}(t) = x\left[z - Ax^2 + g(x,y)\right], \tag{4a}$$

$$\dot{z}(t) = \gamma(1 - z - x^2) + F(t), \tag{4b}$$

$$\dot{y}(t) = y\left[v - Ay^2 - h(x,y)\right], \tag{4c}$$

$$\dot{v}(t) = \gamma(1 - v - y^2) + F(t), \tag{4d}$$

where (x, z) and (y, v) are state variables of two coupled subsystems, and the functions g and h are described as

$$g(x,y) = -By^2 + 4(B - A)\alpha y^2\left[1 - \frac{2y^4}{(x^2 + y^2)^2}\right], \tag{5a}$$

$$h(x,y) = Bx^2 + 4(B - A)\alpha x^2\left[1 - \frac{2x^4}{(x^2 + y^2)^2}\right]. \tag{5b}$$

This oscillatory model was used to simulate visual perception of ambiguous images, such as a Rubin vase. The pair of variables (x, y) is related to the perception of different interpretations of the bistable image, corresponding to two different orientations of the Necker cube, and the other pair (z, v) corresponds to the effect of attention saturation. The functions $g(x, y)$ and $h(x, y)$ describe the asymmetric nonlinear mutual coupling in the corresponding subsystems. In the model, a special role belongs to the damping mechanism that imitates the saturation effect and synaptic connections. Finally, α is the shift parameter relating to the preferable perception state, and $F(t) = D\xi(t)$ is a random variable with the amplitude D and $\xi(t) \in [-1, 1]$.

The deterministic system (4) at $F = 0$ demonstrates alteration of regimes from periodic at $\alpha \in (0, 0.17)$ through the bistability regime of the coexisting periodic orbit and stable equilibrium state ($\alpha \in (0.17, 0.23)$) to the only stable point at $\alpha > 0.23$. When adding noise, the dynamics becomes probabilistic. A weak noise with an intensity of $D < 0.012$ does not lead to intermittency of the dynamics of variables $x(t)$ and $y(t)$ and only changes the statistical properties of the system, ensuring a preference for one dynamic regime over the other. In this case, x and y demonstrate almost regular oscillations, occasionally interrupted by some disturbances at shorter time intervals. When increasing the noise ($0.012 < D < 0.094$), random switchings between different regimes arise. Over a relatively long time, $x(t)$ takes a zero value, while y demonstrates noisy oscillations. From the point of view of ambiguous image perception, the above intervals can be interpreted as the preferable perception of one of two possible interpretations of the Necker cube. With the growth of D, the duration of the intervals of preferable perception increases.

Thus, the oscillatory model shows that additive noise can induce a preference for one of the states. When the noise amplitude exceeds a certain threshold, one of the perceptive states vanishes in regular time intervals, which leads to an interruption of the perception. In this case, the duration of one of the perceptions dominates over the other and grows with increasing noise [143].

3.4 Combined perception model with noise and adaptation

From the above consideration, it is clear that information perception in the brain is generally determined by both adaptation and noise. The adaptation ensures the brain tendency to switch with time between two states of perception, destabilizing the current state. In terms of the above mathematical models, such a deterministic mechanism allows switching between alternating perceptive decisions about the sensory information, characterized by potential wells of comparable depth on the energy landscape. This is important for the brain in order to avoid accepting the first decision (the first 'deep' potential well encountered) as the only correct one. However, the stochastic mechanism enables the brain to easily navigate on the energy landscape, avoiding small potential wells, which can be overcome exclusively by means of noise with a relatively small amplitude.

A drawback of purely attractor and purely oscillatory models is that they incompletely describe real psychophysical experimental data, such as histograms of residence time and correlation between the durations of sequential interpretations of ambiguous images. Therefore, a more exact model of sensory information perception must take into account the following processes [144]:

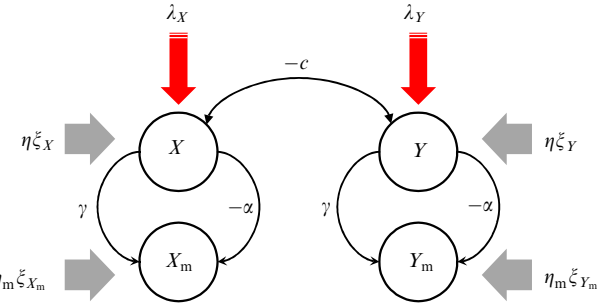

Figure 11. Model of perception with noise and adaptation. Here, X_m and Y_m are states of memory neurons connected by inhibitory connections with perception states X and Y, which in turn also act to inhibit each other, α and γ are the corresponding connection forces, and c is the coefficient of competitiveness of states. Red arrows indicate stimulation effects λ_X and λ_Y, gray arrows indicate noise effects.

• *Self-stabilization*. The ability to support stable perception in the presence of random oscillations of physiological variables (endogenous noise), such as body temperature, blood pressure, and spontaneous activity of neurons, which leads to physiological tremors.

• *Competitive inhibition*. At every moment of time, a person can interpret an ambiguous stimulus in only one possible way and never make two decisions at once; therefore, other decisions are suppressed. Neurons respond only when the input signal is strong enough (otherwise, neurons are 'silent'). Therefore, the sigmoidal function $\sigma(X) = 1/(1 + \exp(-\beta X))$ is used to model synaptic connections under competitive inhibition.

• *Adaptation*. Self-destabilization or spontaneous transitions between perceptive states X and Y from the memory states X_m and Y_m, which are also self-destabilized. The sigmoidal function is also used to reflect the influence of memory on the perception state.

The improved model of perception that takes into account the above requirements is schematically shown in Fig. 11 and is specified by the following equations [144]:

$$\tau\dot{X} = \lambda_X + h - X - c\sigma(Y) - \alpha\sigma(X_m) + \eta\xi_X(t)\,, \tag{6a}$$

$$\tau_m\dot{X}_m = h_m - X_m + \gamma\sigma(X) + \eta_m\xi_{X_m}(t)\,, \tag{6b}$$

$$\tau\dot{Y} = \lambda_Y + h - Y - c\sigma(X) - \alpha\sigma(Y_m) + \eta\xi_Y(t)\,, \tag{6c}$$

$$\tau_m\dot{Y}_m = h_m - Y_m + \gamma\sigma(Y) + \eta_m\xi_{Y_m}(t)\,, \tag{6d}$$

where X and Y are the states of perceptive neurons, X_m and Y_m are the memory states, λ_X and λ_Y are the input signals, α is a coefficient related to the adaptation strength, γ is the memory strength which determines how strongly the choice of the current state affects the memory, τ and τ_m are coefficients of time scaling, h and h_m are the rest potentials for perceptive states and the operative memory, respectively, without external stimulation, and c is the coefficient of competitiveness, which represents the strength of the 'winner' state suppressing the 'loser' state. The ratio of λ_X and λ_Y is determined by the stimulus ambiguity. When the stimulus is completely ambiguous (like the symmetric Necker cube), we are dealing with a nonbiased signal, i.e., $\lambda_X = \lambda_Y$. Brain endogenous noise is added to the variables of perception and memory in the form of independent zero-mean Gaussian noise ξ with the intensities η and $\eta_m = \sqrt{\tau/\tau_m}\eta$, respectively.

In the present model, the noise significantly affects the relative values of X and Y, which, in turn, determine the

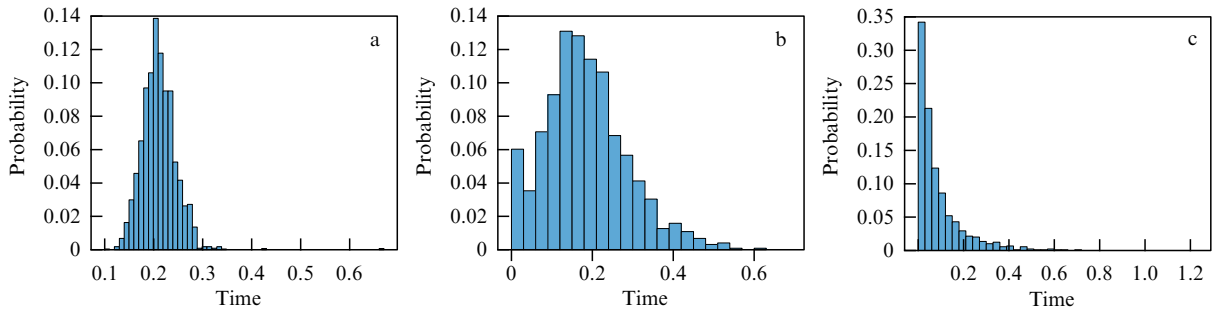

Figure 12. Probability distributions of residence time in one perceptive state at noise intensity $\eta = 0.1$ (a), $\eta = 0.3$ (b), and $\eta = 1$ (c).

magnitude of competitive inhibition between two perception states. Sooner or later, this leads to switching between these states due to the adaptation mechanism. Hence, from the point of view of an exterior observer, the trajectory randomly switches between two perceptive states.

An important characteristic of ambiguous visual object perception is the time spent by the system in one of the perceptive states, the so-called residence time T_R. In model (6), this is described as domination of one of the variables, i.e., one state is specified by the condition $X > Y$ and the other by $Y > X$. Figure 12 shows the probability distributions of T_R for three different values of noise intensity. When the noise is weak, the distribution is almost Gaussian (Fig. 12a), whereas for medium noise levels it is close to the gamma distribution (Fig. 12b), which is typical of biological systems. Finally, for strong noise, the distribution becomes exponential (Fig. 12c). The modeling also shows that the duration in one state or another decreases as noise intensity grows. This agrees well with the experimental data on bistable perception [145, 146].

In experiments on bistable image perception, Meilikhov et al. [147] found that brain noise provides only 15–40% of the difference between the depth of potential wells among the participants of the experiment [136] described in Section 3.3, if assessing them within the attractor model (3). This is an additional argument in favor of the combined model, demonstrating that the adaptation effect dominates in a number of cases over the noise effect.

Therefore, the combined model of perception allows for the activity of all feature-representing neurons in each hemisphere and does not consider spatial variations across the surface. In spite of multiple simplifications, this model is suitable for a qualitative description of many neurophysiological experiments. For example, the most popular method of neuroimaging, electroencephalography (EEG), often records electric activity of neurons in the visual cortex of two hemispheres using only two channels (O_1 and O_2) [148, 149]. Other noninvasive methods of neuroimaging, such as MEG, functional near-infrared spectroscopy (fNIRS), and functional magnetic resonance imaging (fMRI), do not possess super-high spatial resolution accessible in invasive studies, when electrodes are implanted directly in neuron cells.

4. Methods of brain noise measurement

4.1 Experimental assessment of brain noise from behavioristic data based on psychometric functions

In psychophysical experiments, the characteristic that is easy to measure is the psychometric function. Psychometric functions describe the relation between the presented stimulus and the human response to this stimulus and are the probabilities of detecting (recognizing) stimuli as a continuous function of level, intensity, or type of the stimulus. The most widespread and interesting for investigation is the sigma-like psychophysical function, reflecting the observer's behavior near the perception threshold. This occurs because the transition from one reaction to another (e.g., from 'cannot classify the stimulus' to 'can classify the stimulus') is not instantaneous. Since neural reactions are volatile, including due to the noise of the neural ensemble [30, 34], subjects do not similarly respond to each stimulus, especially near the perception threshold. As a consequence, the psychometric function can serve as an effective indirect characteristic for assessing the stochastic properties of neural responses, recorded by the nature of a person's interpretation of sensory information as a response to a certain series of stimuli presented to him or her.

Let us consider an approach to measuring brain noise based on the measurement of psychometric functions. The authors of Ref. [150] proposed an experimental technique based on the specific features of brain operation during the interpretation of bistable images. The main idea of the method was to present to the subject bistable images with different degrees of ambiguity, which acts as a continuously changing stimulus type in the course of constructing the psychometric curve. The authors of Ref. [150] used the experimental paradigm with an ambiguous bistable visual stimulus in the form of a Necker cube allowing two possible interpretations (Fig. 9a). Obviously, those images that have a low degree of ambiguity are interpreted correctly almost always. At the same time, bistable images with a high degree of ambiguity are interpreted in a different way with a certain degree of probability. So, it is possible to construct the psychometric function by presenting to the subject a set of images with different degrees of ambiguity g and measuring the probability to choose this or that interpretation of the bistable image.

In the experiment, images of a Necker cube with $N = 16$ degrees of ambiguity $\Delta g_i = g_i - g_0$ (the contrast parameters being $g_i = i/(N-1)$ ($g_0 = 0.5$, $i = 0, \ldots, N-1$) for faces *1–2–3* and $1 - g_i$ for faces *4–5–6*, as shown in the inset of Fig. 10a) were shown to the subject on a screen 750 times in a random sequence. The subjects were asked to press the left or right key on a double-key keyboard according to their first visual impression (left- or right-oriented cube). For each value of g_i, the probability $P_r(g_i)$ of a right-oriented cube (pressing the right key) was calculated as

$$P_r(g_i) = \frac{p_r(g_i)}{p_r(g_i) + p_l(g_i)}\,, \tag{7}$$

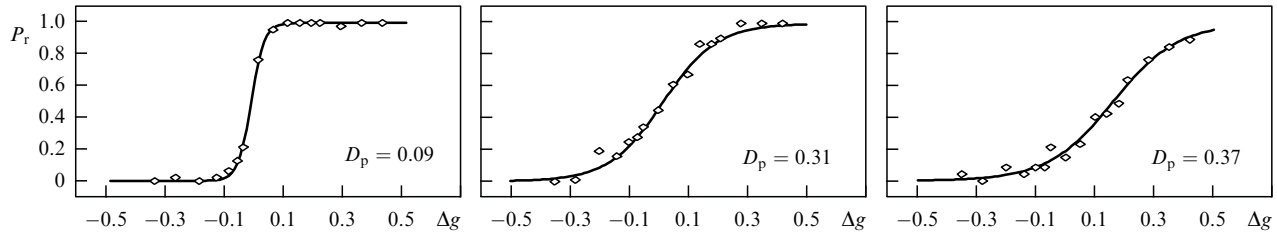

Figure 13. Experimental (diamonds, Eqn (7)) and theoretical (curves, Eqn (16)) psychometric functions for subjects with different levels D_p (18) of endogenous brain noise during perception of Necker cubes with various degrees of ambiguity.

where $p_r(g_i)$ and $p_l(g_i)$ are the numbers of times the right and left keys are pressed in response to the presented stimulus with the ambiguity degree g_i.

In Fig. 13, the diamonds show experimental psychometric functions measured in several subjects. Differences in the slope of the curves in the vicinity of the maximum degree of ambiguity $\Delta g_i \approx 0$ are clearly seen. This fact demonstrates that each subject is characterized by their own level of neural noise. Is it possible to determine it quantitatively?

The perception of an ambiguous image leads to random oscillations in the interpretation; therefore, a symmetric Necker cube ($g = 0.5$) during the observation is perceived alternatingly as a left- or right-oriented cube. Such alternation of two possible interpretations of an ambiguous stimulus indicates the fact that the system is close to an assembly-type catastrophe [151], near which a bistable system is described by a dimensionless potential energy function with two local minima $x_{l,r}$ [104]:

$$U(x) = \frac{x^4}{4} - \frac{x^2}{2} + \frac{\Delta g}{\alpha}\, x\,, \tag{8}$$

where α is the scale factor determined by individual features of the potential profile with two wells, and the dimensionless activity x of the neural population can be written as

$$\dot{x} = -U'(x) + \xi(t)\,, \tag{9}$$

where $\xi(t)$ is δ-correlated Gaussian noise with $\langle \xi_n \rangle = 0$ and $\langle \xi_n \xi_m \rangle = D\delta(n-m)$ (D being the noise intensity).

The noise in Eqn (9) leads to the stochastic differential equation

$$\mathrm{d}X = -U'(x)\,\mathrm{d}t + \mathrm{d}W\,, \tag{10}$$

where $X(t)$ and $W(t)$ describe stochastic one-dimensional Wiener processes. The probability density $\rho_X(x,t)$ of the stochastic process $X(t)$ can be described by the Fokker–Planck equation

$$\frac{\partial \rho_X(x,t)}{\partial t} = \frac{\partial}{\partial x}\left[U'(x)\rho_X(x,t)\right] + \frac{D}{2}\,\frac{\partial^2 \rho_X(x,t)}{\partial x^2}\,. \tag{11}$$

Since the stationary probability density $\rho(x)$, which is a solution to Eqn (11), does not depend on time, Eqn (11) can be reduced to the ordinary differential equation

$$\rho'(x) + \frac{2}{D}\,U'(x)\,\rho(x) - C = 0\,, \tag{12}$$

from which we obtain a general form of the stationary probability density $\rho(x)$, which is a solution to the Fokker–Planck problem (11) [104]:

$$\rho(x) = \exp\left(-\frac{2U(x)}{D}\right)\left[A + C\int_0^x \exp\left(\frac{2U(z)}{D}\right)\mathrm{d}z\right], \tag{13}$$

where A and C are unknown constants. Having found the constant C from the extremum condition $\rho'(x_{l,r}) = C = 0$, we obtain the stationary density function in the final form:

$$\rho(x) = A\exp\left(-\frac{2U(x)}{D}\right), \tag{14}$$

where A is determined by the normalization condition

$$\int_{-\infty}^{\infty} \rho(x)\,\mathrm{d}x = 1\,. \tag{15}$$

In the case of a symmetric ambiguous stimulus, for example, in the Necker cube experiment, the probability that the subject will perceive one of two possible interpretations, e.g., the right cube orientation, can be calculated as

$$\hat{P}_r = \int_0^{\infty} \rho(x)\,\mathrm{d}x\,, \tag{16}$$

where $\hat{P}_r$ is determined by the parameters Δg, α, and D. Fixing α and D and using Δg as a control parameter, it is possible to calculate the probability $\hat{P}_r(\Delta g, \alpha, D)$ of image perception as the right-oriented cube and to compare it with the experimental psychometric function (7). The values of α and D in Eqn (16) can be found by means of the least squares method to minimize the error:

$$E(\alpha, D) = \sum_{j=1}^{N}\left[P_r(\Delta I_j) - \hat{P}_r(\Delta I_j, \alpha, D)\right]^2. \tag{17}$$

As was shown in Ref. [150], the minimum error $E_{\min}$ corresponding to the best coincidence of theoretical and experimental results is approximated as follows:

$$\alpha D = D_p = \mathrm{const}\,. \tag{18}$$

In other words, the parameter D_p is a universal invariant that ensures the minimum $E_{\min}$ on the surface of error values $E(\alpha, D)$. Correspondingly, the value of D_p can be interpreted as the effective noise intensity related to the individual potential well $U(x)$ (8). This effective noise intensity D_p can be easily determined from the psychometric function by the least squares method and should be considered to be closely related to the individual specific features of human perception. A comparison of the experimental data and theoretical

studies (see Fig. 13) demonstrates perfect agreement of the theoretical prediction (solid line) with the experimentally obtained points.

4.2 Brain noise assessment by processing sensory information from EEG/MEG data

Brain noise can also be assessed directly from experimental data on neuroimaging, first and foremost, from recorded electroencephalograms (EEGs) and magnetoencephalograms (MEGs). Multiple data on neurophysiological activity indicate the presence of a strong stochastic component, or $1/f$ noise (flicker noise), in the EEG power spectrum [152, 153]. The noise spectral density in this case corresponds to the power law $S(f) = C/f^{\alpha}$. In Ref. [154], a wavelet analysis was used to estimate $S(f)$ in the frequency F range of interest, which then was approximated by a power law. The noise intensity I was calculated in this case as an integral,

$$I = \int_{f \in F} \frac{C}{f^{\alpha}} \, \mathrm{d}f, \tag{19}$$

where the parameters C and α were found by approximating the experimental EEG wavelet spectra by the least squares method.

In Ref. [155], the unbiased sample variance s^2 was used to estimate noise from the EEG:

$$s^2 = \frac{1}{m-1} \sum_{i=1}^{m} (x_i - \bar{x}) \,, \tag{20}$$

where x_i is the EEG signal under study, m is the number of counts of the signal in the studied time series, and $\bar{x}$ is the mean value. The coefficient $1/(m-1)$ is taken instead of $1/m$ due to using the Bessel correction. Here, it should be noted that approaches (19) and (20) are more convenient to assess the brain endogenous noise from the EEG/MEG signals at rest, whereas for assessment of perception and processing sensory information it is necessary to take into account the individual specific features of brain functioning.

One efficient method to assess neural noise is based on the frequency fixation of the brain's reaction to a periodically modulated stimulus [123]. As known from the theory of coupled oscillators [156], in a stochastic or chaotic system subjected to a periodic external force, frequency locking (synchronization) is possible in a certain frequency range. Frequency locking can either be continuous or exhibit intermittent behavior, depending on both the amplitude of the external stimulus and the intensity of the noise. In the intermittency mode, synchronization windows are interrupted by jumps in the phase difference between the signals of the oscillator ensemble and the external force by $2\pi n$ ($n = \pm 1, \pm 2, \ldots$). At the same time, in the synchronization mode, the phase difference is not completely synchronized, but due to noise it fluctuates around the average value. The amplitude of these phase oscillations is determined by the intrinsic noise of the brain: the stronger the noise, the greater the amplitude of the phase oscillations.

The experimental technique of brain noise assessment was as follows [123]. The subjects were shown a blinking visual stimulus at a frequency of $f_{\mathrm{s}} = 6.67$ Hz. Simultaneously, the MEG was recorded. Since the blinking frequency is high enough to prevent returning the evoked neural activity to the initial state, the evoked brain response was continuous. In the case of a MEG, such a response is called the steady-state visual evoked field (SSVEF). A spectral analysis shows that the maximum SSVEF response corresponds to the second harmonic of the visual stimulus modulation frequency, i.e., to $2f_{\mathrm{s}} = 13.34$ Hz. The phase difference between SSVEF and the second harmonic of the stimulation signal was measured as

$$\Phi = \left(t_n^{\mathrm{b}} - t_n^{\mathrm{s}}\right) 2f_{\mathrm{s}} \,, \tag{21}$$

where t_n^{b} and t_n^{s} are the time positions of the nth maximum of brain reaction (SSVEF) and the second harmonic of the blinking signal, respectively.

The SSVEF phase fluctuations in temporal windows where the phase is fixed were used for statistical analysis. Figure 14 shows examples of the probability distribution of SSVEF phase fluctuations in one of the subjects and the kurtosis coefficients K for eight participants, calculated by the formula

$$K = \frac{\mathbb{E}(\Phi - \mathbb{E}\Phi)^4}{\sigma^4} \,, \tag{22}$$

where σ is the standard deviation of the SSVEF phase fluctuation and $\mathbb{E}$ is the expectation value. Since the noise is related to a wider phase probability distribution, the reciprocal kurtosis coefficient can be a quantitative measure of noise [123].

The neural noise recorded experimentally is a result of random neurophysiological activity of the neural network, whereas the noise of attention concentration leads to SSVEF

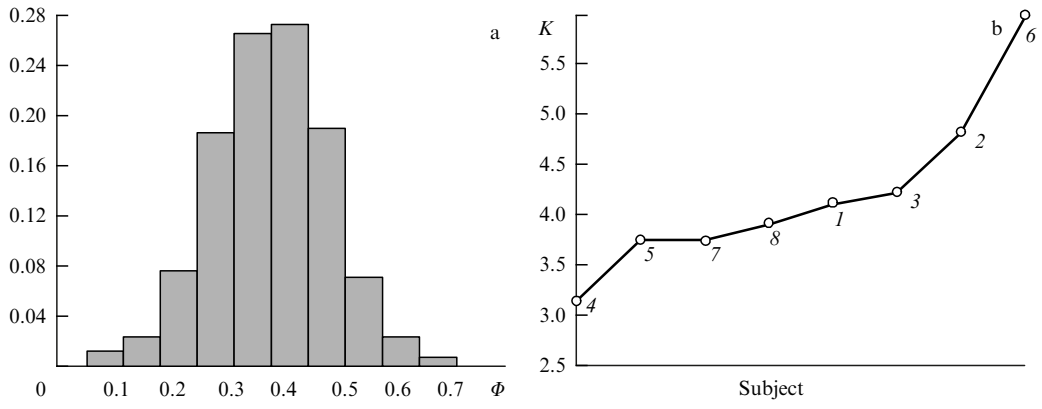

Figure 14. (a) Probability distribution of the SSVEF phase difference for one of the subjects and (b) kurtosis coefficient for the eight subjects participating in the MEG experiment. Participants with a higher kurtosis coefficient have less brain noise. (Adapted from [123].)

phase jumps. In our paper [157], a linear positive correlation was found between the mean power of the neural activity sources in the visual cortex and brain noise. The results show that subjects with a higher power of visual cortex activity demonstrate more substantial brain noise. This interrelation can be explained by the fact that the higher the power of reconstructed sources, the more neurons involved in the realization of cognitive activity and, therefore, the noise is higher in a larger neural network (see Section 2.3).

Since the cortical neural network of each individual is unique, the knowledge of brain noise may be useful for developing efficient brain–computer interfaces [158], adapted to the brain noise of the subject. Indeed, as was shown in Section 3.1, the size of the neural network and, correspondingly, the brain noise adapt to obtain a coherence resonance regime which allows improving the perception of weak stimuli and connections between the neurons. The experiments described in Section 3.1 have shown a possibility of controlling brain noise by means of external stochastic stimulation of the brain. In the future, such stimulation could be used in special neurointerfaces for controlling the neural noise in order to obtain an external coherence or stochastic resonance to help a person perceive weak stimuli and more efficiently process sensory information.

5. Applications of brain noise concept in biomedical studies

As we already discussed above, brain noise is determined by random background electric oscillations in the central nervous system as a result of random misactivation of the nervous system [159–161]. Since incoming sensory stimuli are encoded in the brain by neural impulses, they are processed against the background of neural noise, which depends, along with other factors, on the condition of the nervous system. The noise can be considered in comparison with the signal level for relevant or actively processed information; the nervous system demonstrates a high level of noise if the ratio of the signal power to the power of random background noise is low. Brain noise can appear when the connections between neurons are weakened or degraded as a result of reduced branching, loss of neurons, or periodic inhibition [162]. Brain noise that is too strong or too weak can be a consequence of some mental diseases such as autism or schizophrenia. Increased noise can precede pathological brain conditions, e.g., epileptic discharges. In addition, the brain noise changes with age, as well as a result of neurodegenerative diseases, such as Alzheimer's disease. Hence, brain noise can serve as a biomarker, indicating the risk of development of the above diseases. Let us consider these issues in more detail.

5.1 Autistic spectrum disorders

Autistic spectrum disorder (ASD) is a disorder of nervous system development characterized by a deficiency of social communication and language skills, as well as limited interests and repeated behavior. Greg Davis and Kate Plaisted-Grant [163] formulated a hypothesis that people with ASD have endogenous brain noise that is too low. This hypothesis was based on the high variability in EEG records in patients with ASD [164]. The low level of endogenous neural noise with autism can provide attractive heuristics for explaining a number of ASD features, including its clinically apparent symptoms and the results of a number of laboratory studies.

Such a behavior is likely related to the fact that patients with ASD use relatively small regions of the brain's neural network to solve cognitive problems; therefore, the number of neurons and synaptic connections involved in information processing is not large. The attractiveness of this hypothesis consists in the fact that it helps in understanding the atypical structural and functional connections in the case of autism [165–167]. Notably, patients carrying a widespread version the MET gene, linked with autism, have an abnormally low degree of structural connections in the brain, the effect being particularly expressed in children with ASD. Similarly, patients with ASD have fewer functional connections between distal regions of the brain and more in proximal brain regions [168]. In Ref. [169], for girls with Rett's syndrome, a hard disorder of nervous and mental development classified as ASD, the far temporal correlations measured by the fluctuation analysis method applied to EEG signals in the range of 6–13 Hz were shown to considerably increase as compared to a healthy group of typically developing children. This fact shows a more predictable character of brain electric activity oscillations and, therefore, a decrease in the intensity of the noise component of EEG signals.

How are functional neural connections and brain noise related? Our studies have shown that the brain noise directly depends on the number of neural connections, since every neuron and every connection contribute to the stochastic component. Simply speaking, the greater the number of connections, the stronger the noise.

Many genes for the potential risk of autism regulate the synaptic connectivity, and mutations lead to a microscopic disconnection of neurons [170]. The analysis of multichannel EEGs at rest in groups of relatives (twins, brothers, and sisters) based on the diagnostics of functional networks within the frameworks of the graph-theoretical paradigm of small-world network locking [171] allowed a conclusion that 37–62% of differences in the length of functional connections are hereditary [172]. The clustering coefficient showed that genetics exert a similar influence, since 46–89% of individual differences turned out to be hereditary. A high inheritance of structural parameters of the small-world networks opens up a possibility of further considering them as ASD endophenotypes or ASD risk. However, it is also worth noting that many inherited genes and genes taking part in the 'monogenic' forms of syndromic ASD converge on common paths, which participate in synaptic development, plasticity, and signal transmission [173]. Hence, although the inherited features of the brain network organization are promising as risk biomarkers, they are incomplete endophenotypes of ASD risk and, moreover, are neutral with respect to particular genetic factors.

Although EEG/MEG experiments have already proved the existence of differences in functional connections between ASD patients and healthy subjects, additional studies are extremely necessary to measure the brain noise and its correlation with structural and functional connections in the brain. For this purpose, it is possible to use the methods described in Section 4. Thus, brain noise can be a good ASD marker.

5.2 Schizophrenia

Another deviation from normal mental health related to an anomalous level of brain noise is schizophrenia. In this area, it is worth mentioning the interesting studies by Winterer et al. [174] from the Free University of Berlin, who back in 2000

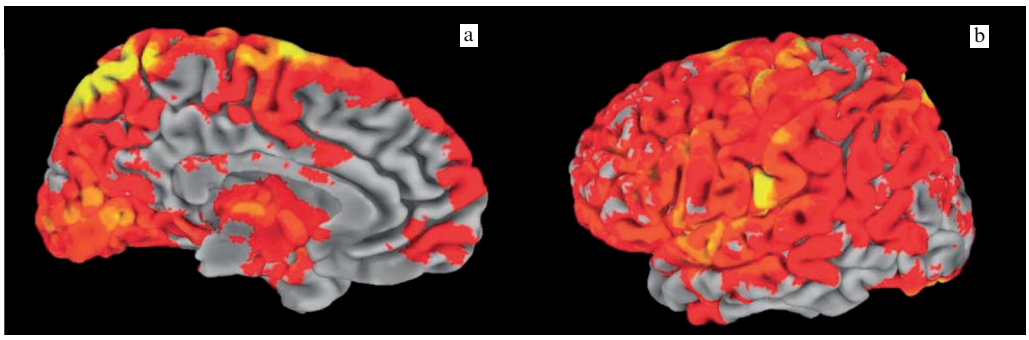

Figure 15. Mapping the cortical surface with group difference mean variance of residual noise. (a) Control group ($N = 14$). (b) Group of patients with schizophrenia ($N = 10$). Areas with high residual noise variance are shown in red. (Based on data from [176].)

discovered an increased level of brain noise in patients with schizophrenia using EEG studies. The researchers measured the auditory reaction time of selecting audio tones of two different frequencies (1000 and 2000 Hz), presented in a pseudo-randomized sequence at an interval of 2.5–7.5 s using loudspeakers at a sound pressure level of 65 dB. The total duration of the task was 5 min. The patient had to turn off the sound as soon as possible by pressing one of two buttons. The signal with a low tone was turned off with the left hand, the high-tone signal, with the right hand. The number of errors, the average response time, and the standard deviation of these characteristics were calculated. Measurements of the stability of mean reaction latency in 20 subjects over a test-retest interval of approximately six months revealed a Cronbach's alpha coefficient of 0.896, indicating the intrinsic consistency of each subject's characteristics [175].

Then, the EEGs of four groups of subjects who had not previously taken medication were compared: Group I of 41 patients with schizophrenia, Group II of 233 healthy people, Group III of 21 patients with schizotypal personality disorder at high risk of schizophrenia, and Group IV of 71 patients with developing schizophrenia and nonmedicated depression. By measuring event-related brain activity during the reaction to the choice of acoustic signal, the signal-to-noise ratio, signal strength, and noise were calculated in a time interval of 50–200 ms after the stimulus was presented. The authors of [174] also carried out a frequency analysis of prestimulus and poststimulus EEGs.

As a result of the study, a reduced signal-to-noise ratio of evoked activity was found in patients with schizophrenia; in schizotypal and depressive subjects, there was a slight downward trend. The observed decrease was shown to be due to a decrease in signal power and an increase in absolute noise power. Frequency analysis of evoked activity revealed increased theta/delta activity between pre- and post-stimulus intervals to the same extent in normal individuals, schizophrenics, schizotypals, and depressives. However, this increase in the theta/delta ratio in the pre- and post-stimulus intervals did not correlate with signal strength in patients with schizophrenia. Additionally, there was an increase in coherence between both temporal lobes in healthy and depressed subjects during information processing, which was not found in patients with schizophrenia and schizotypal disorder. On the contrary, in the latter two groups, frontal lobe coherence improved, accompanied by increased noise. The observed low signal-to-noise ratio during information processing in patients with schizophrenia is explained by a decrease in stimulus-induced phase synchronization and bitemporal coherence of induced neural activity, rather than by a lack of activation. In other words, in patients with schizophrenia, brain noise increases after the presentation of a stimulus, in contrast to the control group, in which there is an increase in the signal.

More recently, Winterer et al. [176] examined prefrontal response variability of discrete frequency components over a wide frequency range (0.5–45 Hz). Using the odd-ball paradigm, they recorded the EEGs of 66 patients with schizophrenia, 115 of their clinically healthy siblings, and 89 healthy subjects. The odd-ball paradigm is an experimental protocol often used in psychological investigation, in which the subject is presented with a sequence of repeated stimuli, occasionally interrupted by a deviant (strange) stimulus. The experiment records the subject's reaction to the deviant stimulus.

Prefrontal noise was found to be negatively correlated with working memory performance in all subjects. The authors also note that brain noise may be a marker of working memory performance, which is associated with the genetic risk of schizophrenia. Cognitive function associated with the frontal lobe has been found to depend on the ability to synchronize cortical pyramidal neurons, which is partly genetically controlled. The increased prefrontal noise is an intermediate phenotype associated with a genetic predisposition to schizophrenia.

Increased noise in the prefrontal region in patients with schizophrenia has also been found in fluctuations in blood oxygen levels measured using functional magnetic resonance imaging (fMRI), which is one of the most informative tools today for studying the blood supply to the brain. When analyzing fMRI data, doctors and researchers typically filter out noise to identify the useful signal. However, the noise level can also provide important information about cognitive processes, effectively being an indicator of cognitive flexibility.

Figure 15 shows the average residual noise variance in the left medial frontal lobe region determined using fMRI. As can be seen, the average variance of residual noise in subjects of the control group is lower than in patients with schizophrenia. Higher mean variance of residual noise in patients with schizophrenia was also found in a wide area, including the dorsolateral prefrontal, parietal, and occipital cortices, thalamus, and cerebellum.

The increase in noise was found in two of its manifestations: increased residual noise variance and a more diffuse nature (more independent components) of the stimulus-induced response, depending on the level of oxygen in the blood. The analysis showed that both noise manifestations, measured using fMRI, characterized patients with schizophrenia better than the level of prefrontal activation measured using EEG.

Additionally, the blood oxygen level variation increases not only at the level of individual voxels but also across space, as a large number of independent components were found, meaning that the prefrontal blood oxygen level-dependent response pattern is more fractionated. This conclusion was drawn from the frequent observation of reduced functional connectivity in schizophrenia, since the number of independent components can be considered an inverse measure of the degree of functional connectivity of the brain.

5.3 Epilepsy

Recently, scientists have begun to consider spontaneous spike activity in neuronal populations to be an extreme event [177, 178]. In this context, epileptic seizures are especially highlighted as the clearest manifestation of extreme behavior in the neural network of the brain [178–181]. An epileptic seizure is a sudden malfunction of the brain caused by hypersynchronous activity in the functioning of neurons in the neural network of the brain, associated with, among other factors, the effects of explosive synchronization due to changes in the topologies of connections in the neural ensemble [182, 183]. Epileptic seizures can be focal or generalized [184]. Focal seizures occur in a limited area of the brain. In contrast, generalized seizures involve bilaterally and synchronously the two hemispheres, and often the entire brain. Generalized seizures have an obvious clinical electroencephalographic sign — synchronization of non-invasive EEG signals recorded in various distant brain regions.

In [185, 186], extreme event theory was applied to analyze electrocorticogram (ECoG) recordings of rats with a genetic predisposition to absence epilepsy and mice with induced stroke. It has been shown that epileptic seizures are characterized by a sharp increase in wavelet power (WP) in the frequency range of 6–8 Hz. In the specified frequency range, the WP time series exhibit properties associated with extreme events, while at other frequencies no extreme behavior is detected. In the same frequency range, WP exhibits long-range correlations, which is characteristic of systems near the critical point [187], where small fluctuations grow due to destabilization. This effect, known as pre-bifurcation noise amplification, has been observed in various physical, environmental, and biomedical systems [188–191]. Based on these results, the authors of [154] hypothesized that epileptic seizures, like other extreme events, may arise from dynamic instability. Therefore, the intensity of brain noise should increase immediately before an epileptic seizure (preictal state). To confirm this hypothesis, multichannel human EEG signals were examined during secondary generalized epilepsy.

It was also shown in [154] that the time series of EEG wavelet power in the frequency range of 1–5 Hz of an epileptic discharge forms a Weibull distribution with a heavy tail, which reflects the presence of epileptic seizures causing a sharp increase in spectral power in the range of 1–5 Hz. The fact that seizures meet the definition of an extreme event suggests a possible mechanism of occurrence based on dynamic systems theory. The amplification of small disturbances in the EEG signal near the bifurcation is nothing more than an increase in noise arising from the spontaneous activity of neurons. Thus, if the extreme onset of an epileptic event is due to instability, then its development should be accompanied by an increase in noise during the preictal state. To estimate the noise intensity, approaches were used based on both estimating the wavelet power of noise in the range of 1–30 Hz under the assumption that the noise component is described by the C/f^{α}-distribution, and estimating the signal variance in the same frequency range.

Noise intensity values were compared across four windows $(T_1 \dots T_4)$ during the preictal state (Fig. 16a). Figure 16b shows that the average noise intensity increases as the window moves toward seizure onset. Repeated measures correlation analysis was used to quantify the relationship between window number and noise intensity at the group level [192]. This is a statistical method for determining the overall within-individual association for paired measures (noise intensity and number of windows) assessed on two or more occasions $(T_1 \dots T_4)$ for several subjects. The analysis showed a positive relationship, $r_{rm}(29) = 0.52$, $p = 0.002$ (Fig. 16c), which allows a conclusion that the resulting correlation model describes the group data. The result of comparing the signal variance in four windows $(T_1 \dots T_4)$ is illustrated in Fig. 16d. The figure shows that the average signal variance increases towards the beginning of the attack, which is also evidenced by the correlation analysis shown in Fig. 16e ($r_{rm}(29) = 0.38$, $p = 0.031$).

Thus, the presented results show an increase in noise intensity and signal variance before the onset of the attack. It is known that an increase in signal variance is one of the early signs of critical transitions [193], which are a change in the state of a system passing a bifurcation point that corresponds to a critical threshold. When a dynamic system approaches a critical threshold, it experiences what is called critical slowdown, as the system takes time to recover from small disturbances. If a small disturbance develops as $\sim \exp(\lambda t)$, then the maximum Lyapunov exponent λ tends to zero at the critical threshold point. As a consequence, the impact of disturbances does not weaken, and their cumulative effect increases the variance of the state variable.

A number of researchers have also found evidence of a critical transition before the onset of an epileptic seizure. Meisel and Kuehn analyzed pre-attack states at different levels [194]. At the level of individual neurons, they used an analysis based on the FitzHugh–Nagumo model and showed that an increase in variance can be a predictor of spiking activity. They also analyzed the ECoG data and found that the signal variance showed oscillations before the seizure. Chang et al. proposed that epileptic discharges begin due to progressive loss of stability of a neural network governed by the principles of critical moderation [195]. Recently, Maturana et al. also found evidence of critical slowing (increased autocorrelation and variance) of brain activity over short and long time scales [196]. The authors showed that the signal variance experiences fluctuations on various time scales (from hours to days).

The discovered effects of an increase in the noise component of the EEG before an epileptic discharge can be used to predict seizures. The results obtained may also be useful in the development of neural interfaces for the rapid prevention of epileptic discharges in patients [181, 197, 198].

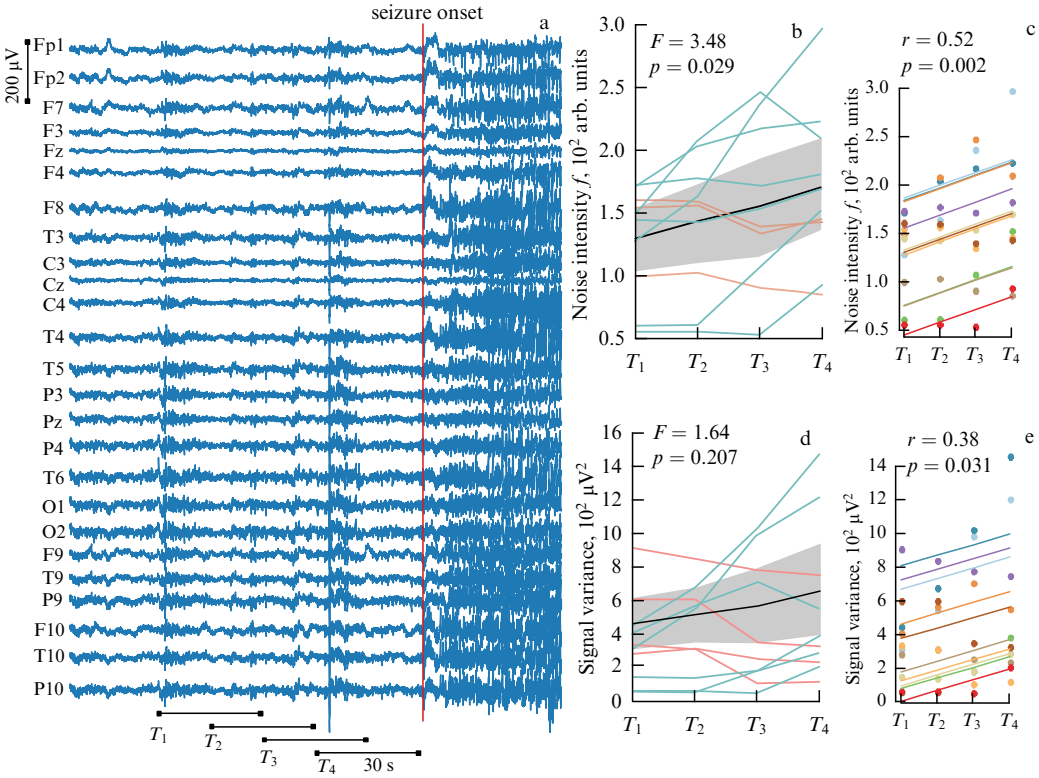

Figure 16. Set of EEG signals, including the preictal period and the onset of an epileptic seizure (vertical solid line). Four horizontal lines $T_1 \ldots T_4$ show the position of time windows used to estimate noise intensity. For each window, it is equal to 30 s. (b) Noise intensity (mean ±95% confidence interval and individual values) estimated for these time windows, $F(3.27) = 3.48$, $p = 0.0029$ using ANOVA. (c) Regression plot: dots correspond to data from each epilepsy patient, lines have the same slope, $r = 0.52$, estimated using repeated measures correlation analysis ($p = 0.002$). (d) Signal variance (mean ±95% confidence interval and individual values) calculated for these time windows, $F(3.27) = 1.64$, $p = 0.207$ using one-way ANOVA. (e) Regression plot: dots correspond to each subject's data, lines have the same slope, $r = 0.38$, calculated using repeated measures correlation analysis ($p = 0.031$). (Figure reproduced with permission from APS © (2021) [154].)

5.4 Influence of narcotic drugs on brain noise

Drugs that cause psychosis can increase brain noise levels, similar to psychotic disorders such as schizophrenia. According to Ref. [199], marijuana consumption increases neural noise in the brain. Marijuana (or cannabis) is the most widely used illicit psychoactive substance worldwide, derived from hemp. The main effect on the human body is exerted by the psychoactive substances (cannabinoids) contained in hemp. The main psychoactive component of cannabis, delta-9-tetrahydrocannabinol (Δ9-THC), causes a number of perceptual changes and cognitive impairments through the activation of cannabinoid receptors in the brain. Neural correlates of cannabinoids can be identified by recording brain electrical activity using EEGs [200].

An experiment by Cortes-Briones et al. [199] involved 24 volunteers who were intravenously administered the main active component of cannabis (Δ9-THC), either a full dose of 0.03 mg kg^{-1} or a half dose of 0.015 mg kg^{-1}, or a placebo in a double-blind, randomized design. The experiment lasted three days, during which acute dose-dependent schizotypal effects were observed. EEG data were recorded with 22 electrodes (sampling frequency of 1000 Hz) during the auditory task. Neural noise was determined by measuring the level of randomness in the EEG during the baseline prestimulus period in the previously described oddball paradigm using the Lempel–Ziv complexity, an efficient and fast algorithm for calculating Kolmogorov complexity, which is a nonlinear measure of the randomness of a signal [201].

The experiment measured behavioral indicators including the percentage of correct responses to target stimuli and the median. The auditory task used three stimuli: a random series of infrequent (8.33%) 'target' tones (1000 Hz), frequent (88.33%) 'standard' click sequences (20, 30, and 40 Hz), and a rare task — irrelevant new distractor sounds (8.33%), presented with a stimulus onset asynchrony of 1.25 s in three separate blocks. New distractor sounds were selected from a set of sounds developed by Friedman et al. [202], which contains a variety of natural and artificial sounds such as barking dogs, car horns, human coughs, and piano sounds. Target tones had a duration of 500 ms and an average sound pressure level of 80 dB. New distractor sounds had a duration of 175 to 250 ms and an average sound pressure level of 80 dB. Standard click sequences had a duration of 500 ms and a sound pressure level of 80 dB. In each block of tasks, subjects were asked to press a response key to target stimuli with the index finger of their preferred hand.

EEG analysis shows that when doses of Δ9-THC that cause a schizotypal effect are administered, neural noise increases in a dose-dependent manner. Additionally, increased neural noise correlates well with the psychosis-like psychotomimetic effects caused by Δ9-THC. It is also of interest to analyze the effect on brain noise of other drugs that cause schizotypal effects, for example, ketamine (an NMDA receptor antagonist) and psilocybin (a serotonin 5HT2A receptor antagonist). If confirmed, brain noise may be useful as a new biomarker of functional deficits underlying schizotypal symptoms. Finally, if schizotypal symptoms are found to

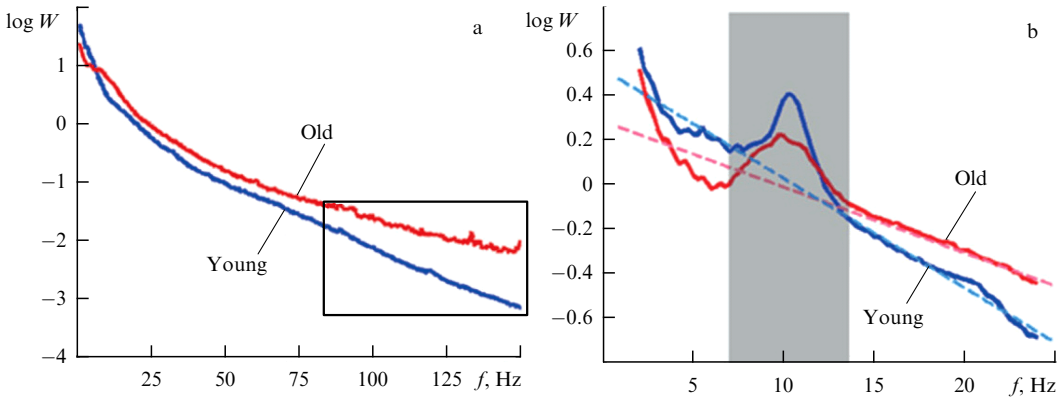

Figure 17. Averaged power spectra of ECoG signals in subjects younger than 21 (blue) and older that 40 (red) demonstrating differences in slope at high frequencies of the gamma rhythm (in black rectangle); at high frequencies, the power is 'smoothed,' which evidences an increase in flicker noise in elderly subjects. (b) Slope of low-frequency power spectrum of EEG signals in the visual cortex region is shallower in elderly patients than in young ones. The flicker noise is assessed by the power spectrum slope (dashed lines) taking no alpha rhythm power into account (gray area, 7–14 Hz). (Based on data from [215].)

result from a disruption in brain connectivity associated with an abnormal increase in neural noise, as is quite possible, then interventions aimed at reducing it (for example, using a brain–computer interface [158] or brain stimulation using electrical or magnetic pulses [203]) may have a potential therapeutic effect.

5.5 Healthy aging and Alzheimer's disease

The concept of neural or intrinsic brain noise to explain age-related differences in information processing has been used for a long time (see, e.g., [204–210]). It is known that the aging brain loses neural connections (see, e.g., [211–213]). This confirms the hypothesis put forward by Crossman and Szafran back in 1955 [214] that the effective signal-to-noise ratio in neural networks decreases with age. It has also been observed that background neural noise increases with age or in disease states (such as Alzheimer's disease, which results in a lower signal-to-noise ratio in older people than in younger people). Thus, a high level of brain noise may be a good indicator of the efficiency of processing incoming information, i.e., it indicates how well connected neural networks are.

To test this hypothesis, a spectral analysis of ECoGs and EEGs was carried out in young and elderly subjects [215]. If, as predicted by the neural noise growth hypothesis, neural impulses are less synchronized in older persons than in younger ones, then this should be reflected in the frequency distribution of spectral power. As is known [111, 112], the characteristic frequency distribution of EEG data corresponds to flicker noise, that is, is inversely proportional to the frequency $1/f$, so the slope of this linear dependence on a logarithmic scale can serve as a measure of neural noise, as shown above (see Eqn (19)), which has greater power at low frequencies than at higher frequencies.

Figure 17a shows the averaged power spectral densities of frontal and temporal cortical intracranial ECoGs. The study involved 15 patients aged 15–53 years with intractable epilepsy who were implanted with subdural electrodes. The recordings were made at three clinics: the Stanford School of Medicine, Johns Hopkins School of Medicine, and University of California, San Francisco. During diagram recording, patients executed auditory passive phoneme listening, word repetition, or auditory attention tasks. It is clearly seen that, in accordance with the hypothesis of an increase in neural noise with age, the slope of the power spectrum in older patients is less than in younger patients.

Although these results support the hypothesis, they should be treated with caution. First, ECoG data were obtained from patients with intractable epilepsy. Second, not all data were used in the analysis; some of the data corrupted by ictal spike activity was removed. Channels with widespread seizure activity were identified by a neurologist or epileptologist and, together with electrodes over areas that were subsequently surgically resected, were excluded from the analysis. It should also be noted that older participants had suffered from epilepsy for a longer period of time, which could have led to long-term neurophysiological changes that could also influence the results.

To address the potential limitations of invasive ECoGs in patients with epilepsy and to better explore the relationship between cognitive processes and flicker noise, non-invasive EEGs were recorded from healthy young (20–30 years old, $N = 11$) and elderly (60–70 years old, $N = 13$) volunteers. Both groups performed a lateralized visual working memory task. Aging is known to be associated with declines in visual working memory and slower reaction times. As can be seen from Fig. 17b, a group of elderly volunteers is characterized by a decrease in power in the theta and alpha ranges (4–14 Hz). The presented results of invasive and non-invasive human electrophysiology convincingly prove that aging leads to an increase in the intensity of $1/f$ brain noise. This is explained by a decrease in the synchrony of neural networks [159, 215–217]. Non-invasive EEG results suggest that age-related changes in $1/f$ noise are associated with cognitive decline affecting working memory. Many researchers studying the relationship between neural noise and aging use response time variability as a proxy metric for neural noise. However, as shown by Voytek et al. [215], it is not response time variability, but rather $1/f$ noise that statistically mediates the relationship between age and a decline in visual working memory. Here, 'mediation' means that the relationship between aging and working memory performance decreases when $1/f$ noise is taken into account, suggesting that the observed correlation between aging and working memory decline is due in part to age-related changes affecting $1/f$ noise.

Analyses of brain activity using fMRI revealed significant differences in the variability of blood oxygen levels between young and elderly subjects [218]. It has been shown that the variability in blood oxygen levels in healthy young adults is significantly greater in certain areas of the brain than that in older adults. Twenty-five young people (from 18 to 25 years old) and 21 older people (from 65 to 85 years old) took part in the experiment. Before the scan, each person had to complete seven tasks designed to test cognitive abilities. In one, the subject was asked to match images by shape or color or to determine as quickly as possible whether two images were different. Another task tested the ability to read aloud. The subjects were also asked to remember pictures of animals shown to them on an iPad and then list them in order of size. These tasks allowed participants to be classified according to their level of cognitive ability. Each person was then given two fMRI scans, during which the participants rested quietly while a snapshot of their brain oxygen levels was taken every two seconds. Before each session, participants were given a low dose of lorazepam, a benzodiazepine known to enhance the effects of gamma-aminobutyric acid (GABA), or a placebo. As a result of the analysis, it was concluded that neural networks find the right balance between inhibition and excitation. When the effect of GABA is small and the inhibition is too weak, the brain becomes overexcited, a large number of neurons are activated, and the network enters a stable state from which it is difficult to recover. Increasing the inhibitory effect of GABA leads the brain to a less excited, more flexible state. Changes in GABA levels in the brain occur in Alzheimer's disease due to the death of nerve cells, causing memory loss. Thus, neural noise acts as a kind of biomarker for how the brain responds to GABA-enhancing drugs. Having a metric-like signal variability that could predict whether a psychiatric drug works or not is very important. Although the development of a drug that slows cognitive decline by targeting neural noise is still a long way off, using noise levels to decide whether a treatment is effective seems feasible.

A number of neuromorphic models show that increased noise with aging is associated with deficits in neuromodulatory systems, leading to decreased neuroplasticity [219] and reduced efficiency of stochastic resonance in stimulus recognition [220].

6. Conclusion

Over the past few decades, biophysical studies of stochastic processes in living systems have attracted the close attention of physicists, mathematicians, and biologists of various specialties, including research in the field of neuroscience. In the present review, we have shown that noise appears at all stages of sensory perception and has a significant impact on perceptual decision making. Without a doubt, brain noise contributes to variability in the responses of the central nervous system and, as a result, in our behavioral responses. However, the contribution of noise compared to the adaptive mechanisms of the nervous system is still not entirely clear. Further study of this issue requires both dedicated experimental studies and stochastic modeling in which each source of variability and noise can be controlled. We discussed in this paper how mathematical models of perceptual choice based on ambiguous sensory information have developed. From the analysis performed, it is obvious that it is impossible to explain the observed experimental facts, whether within the framework of purely stochastic models or within the framework of deterministic models that take into account the effects of plasticity and adaptation of the nervous system. As a result, the most promising models of perception are those in which the above factors (noise and adaptation) are present simultaneously, which makes it possible to describe the phenomena of sensorimotor integration in the neural network of the brain most accurately.

Although noise (including neural ensembles) is traditionally perceived as a negative factor that interferes with functioning, it should be noted that the brain has evolved in conditions where stochastic processes are an inevitable companion to its work. Consequently, the brain has 'learned' to work under conditions of permanent noise influence on all its information processing activity. An interesting idea is proposed in review [34] that the noise level sets both hard limits for the central nervous system, in particular, the degree of miniaturization of neurons (see Section 2.2, which discussed the noise limit of the axon diameter), and soft limits, such as metabolic costs or the amount of time required to complete a task. For example, action potentials are noisy and at the same time metabolically expensive (the average rate of action potential generation of neurons in the cerebral cortex appears to be limited by energy reserves [221]). Therefore, although communication between neurons becomes more reliable due to the use of more action potentials, it simultaneously becomes more energetically expensive. Therefore, in noncritical situations, the accuracy of signal transmission can be sacrificed. However, in tasks critical to the body, a compromise between these factors is necessary. For example, such a compromise is realized in the visual systems of mammals [222–224]. Thus, the noise level acceptable to perform a task depends on the required intrinsic (e.g., accuracy of environmental information or long-term memory stability) and behavioral (e.g., motor accuracy) characteristics. In this context, neural noise is integral to the trade-off between CNS resources (mass, size, etc.) and performance that may ultimately determine evolutionary fitness.

This work also shows that brain noise is a natural manifestation of its dynamics. Brain noise is necessary for information processing; one of the positive effects of noise is coherence resonance, which increases the signal-to-noise ratio at certain (usually threshold) stimulus intensities, which is important in tasks of detecting weak signals. However, it is possible to highlight a more constructive role of noise in the central nervous system: it leads to probabilistic behavior, which is beneficial when making decisions, since it prevents 'deadlocks' in decision making. Finally, in this article we discussed how decision-making can be shaped by stochastic dynamic effects, including the role of noise in enabling probabilistic 'jumps' across potential barriers in the energy landscape describing the dynamics of multistable systems.

This study was supported by the Ministry of Education and Science of the Russian Federation within the Priority 2030 program.

References

1. Trubetskov D I, Mchedlova E S, Krasichkov L V *Vvedenie v Teoriyu Samoorganizatsii Otkrytykh Sistem* (Introduction to the Theory of Self-Organization in Open Systems) (Moscow: Fizmatlit, 2005)
2. Knobloch E *Nonlinearity* **21** (4) T45 (2008)
3. Goldbeter A *Philos. Trans. R. Soc. A* **376** 20170376 (2018)

4. Belintsev B N *Sov. Phys. Usp.* **26** 775 (1983); *Usp. Fiz. Nauk* **141** 55 (1983)
5. Kerner B S, Osipov V V *Sov. Phys. Usp.* **33** 679 (1990); *Usp. Fiz. Nauk* **160** (9) 1 (1990)
6. Medvinskii A B et al. *Phys. Usp.* **45** 27 (2002); *Usp. Fiz. Nauk* **172** 31 (2002)
7. Vanag V K *Phys. Usp.* **47** 923 (2004); *Usp. Fiz. Nauk* **174** 991 (2004)
8. Nekorkin V I *Phys. Usp.* **51** 295 (2008); *Usp. Fiz. Nauk* **178** 313 (2008)
9. Budaev V P, Savin S P, Zelenyi L M *Phys. Usp.* **54** 875 (2011); *Usp. Fiz. Nauk* **181** 905 (2011)
10. Zemskov E P *Phys. Usp.* **57** 1035 (2014); *Usp. Fiz. Nauk* **184** 1149 (2014)
11. Strelkova G I, Anishchenko V S *Phys. Usp.* **63** 145 (2020); *Usp. Fiz. Nauk* **190** 160 (2020)
12. Schlosshauer M *Phys. Rep.* **831** 1 (2019)
13. Anishchenko V S et al. *Phys. Usp.* **42** 7 (1999); *Usp. Fiz. Nauk* **169** 7 (1999)
14. Klimontovich Yu L *Phys. Usp.* **42** 37 (1999); *Usp. Fiz. Nauk* **169** 39 (1999)
15. Mantegna R N, Spagnolo B *Phys. Rev. Lett.* **76** 563 (1996)
16. Parrondo J M R et al. *Physica A* **224** 153 (1996)
17. Ghodrati M *Phys. Rev. D* **98** 106011 (2018)
18. Gursoy M C, Nasiri-Kenari M, Mitra U *Digital Signal Process.* **124** 103161 (2022)
19. Wang B-X et al. *npj Quantum Inf.* **4** 52 (2018) https://doi.org/10.1038/s41534-018-0102-2
20. Yu D et al. *Chaos Solitons Fractals* **157** 111929 (2022)
21. Guérin P A, Rubino G, Brukner Č *Phys. Rev. A* **99** 062317 (2019)
22. Deco G, Romo R *Trends Neurosci.* **31** (11) 591 (2008)
23. Biondo A E et al. *PloS ONE* **8** (7) e68344 (2013) https://doi.org/10.1371/journal.pone.0068344
24. Kolmogorov A N *Usp. Matem. Nauk* (5) 5 (1938)
25. Khinchin A Ya *Usp. Matem. Nauk* (5) 42 (1938)
26. Slutskii E E *Izbrannye Trudy*: *Teoriya Veroyatnostei, Matematicheskaya Statistika* (Selected Works: Probability Theory, Mathematical Statistics) (Moscow: Izd. AN SSSR, 1960)
27. Tolhurst D J, Movshon J A, Dean A F *Vision Res.* **23** 775 (1983)
28. Schuster H G, Just W *Deterministic Chaos. An Introduction* 4th rev. enlarg. ed. (Weinheim: Wiley-VCH Verlag, 2005)
29. Marder E, Goaillard J-M *Nat. Rev. Neurosci.* **7** 563 (2006)
30. Muotri A R, Gage F H *Nature* **441** 1087 (2006)
31. Marder E *Proc. Natl. Acad. Sci. USA* **108** (suppl._3) 15542 (2011)
32. Renart A, Machens C K *Curr. Opin. Neurobiol.* **25** 211 (2014)
33. Stein R B, Gossen E R, Jones K E *Nat. Rev. Neurosci.* **6** 389 (2005)
34. Faisal A A, Selen L P J, Wolpert D M *Nat. Rev. Neurosci.* **9** 292 (2008)
35. McDonnell M D, Ward L M *Nat. Rev. Neurosci.* **12** 415 (2011)
36. Bialek W *Annu. Rev. Biophys. Biophys. Chem.* **16** 455 (1987)
37. Bialek W, Setayeshgar S *Proc. Natl. Acad. Sci. USA* **102** 10040 (2005)
38. Lillywhite P G, Laughlin S B *Nature* **277** 569 (1979)
39. Cover T M, Thomas J A *Elements of Information Theory* (New York: John Wiley and Sons, 1991) p. 279, https://doi.org/10.1002/0471200611.ch12
40. Baddeley R, Hancock P J, Földiák P (Eds) *Information Theory and the Brain* (Cambridge: Cambridge Univ. Press, 2000)
41. Mainen Z F, Sejnowski T J *Science* **268** 1503 (1995)
42. De Ruyter van Steveninck R R et al. *Science* **275** 1805 (1997)
43. Hofmann V, Chacron M J *Front. Integr. Neurosci.* **12** 56 (2018)
44. Saxena S, Cunningham J P *Curr. Opin. Neurobiol.* **55** 103 (2019)
45. Rieke F et al. *Spikes*: *Exploring the Neural Code* (Cambridge, MA: MIT Press, 1999)
46. Bair W *Curr. Opin. Neurobiol.* **9** 447 (1999)
47. Panzeri S et al. *Neuron* **29** 769 (2001)
48. Billimoria C P et al. *J. Neurosci.* **26** 5910 (2006)
49. van Gils T et al. *Neural Comput.* **31** 1789 (2019)
50. Häusser M, Spruston N, Stuart G J *Science* **290** 739 (2000)
51. Stuart G J, Häusser M *Nat. Neurosci.* **4** 63 (2001)
52. Fairhall A L et al. *Nature* **412** 787 (2001)
53. Weber A I, Fairhall A L *Curr. Opin. Neurobiol.* **58** 135 (2019)
54. Zhurov Yu, Brezina V *J. Neurosci.* **26** 7056 (2006)
55. Sober S J et al. *Trends Neurosci.* **41** 644 (2018)
56. Bialek W et al., in *Advances in Neural Information Processing Systems 2. NIPS Conf., Denver, Colorado, USA, November 27–30, 1989* (Ed. D S Touretzky) (San Francisco, CA: Morgan Kaufmann Publ. Inc., 1990) p. 36
57. Cover T M *Elements of Information Theory* (New York: John Wiley and Sons, 1999)
58. Softky W R, Koch C *Neural Comput.* **4** 643 (1992)
59. Tomko G J, Crapper D R *Brain Res.* **79** 405 (1974)
60. Gur M, Beylin A, Snodderly D M *J. Neurosci.* **17** 2914 (1997)
61. DeWeese M R, Wehr M, Zador A M *J. Neurosci.* **23** 7940 (2003)
62. Azouz R, Gray C M *J. Neurosci.* **19** 2209 (1999)
63. Deco G, Hugues E *PLoS Comput. Biol.* **8** (3) e1002395 (2012)
64. Huang C et al. *Neuron* **101** 337 (2019)
65. Schneidman E, Freedman B, Segev I *Neural Comput.* **10** 1679 (1998)
66. White J A, Rubinstein J T, Kay A R *Trends Neurosci.* **23** (3) 131 (2000)
67. Yu H et al. *Physica A* **471** 263 (2017)
68. Faisal A A, White J A, Laughlin S B *Curr. Biol.* **15** 1143 (2005)
69. Faisal A A, Laughlin S B *PLoS Comput. Biol.* **3** (5) e79 (2007)
70. Cecchi G A et al. *Proc. Natl. Acad. Sci. USA* **97** 5557 (2000)
71. Fellous J-M et al. *Neuroscience* **122** 811 (2003)
72. Rusakov D A, Savtchenko L P, Latham P E *Trends Neurosci.* **43** (6) 363 (2020)
73. Stuart G J, Sakmann B *Nature* **367** 69 (1994)
74. Stevens C F, Zador A M *Nat. Neurosci.* **1** 210 (1998)
75. Wehr M, Zador A M *Nature* **426** 442 (2003)
76. Wang S-Q et al. *Nature* **410** 592 (2001)
77. Lou X, Scheuss V, Schneggenburger R *Nature* **435** 497 (2005)
78. Bekkers J M, Richerson G B, Stevens C F *Proc. Natl. Acad. Sci. USA* **87** 5359 (1990)
79. Zucker R S, Regehr W G *Annu. Rev. Physiol.* **64** 355 (2002)
80. Redman S *Physiol. Rev.* **70** (1) 165 (1990)
81. Jack J J B et al. *Cold Spring Harb. Symp. Quant. Biol.* **55** 57 (1990)
82. Sylantyev S et al. *Proc. Natl. Acad. Sci. USA* **110** 5193 (2013)
83. Jensen T P et al. *Nat. Commun.* **10** 1414 (2019)
84. Sulzer D, Edwards R *Neuron* **28** (1) 1 (2000)
85. Wu X-S et al. *J. Neurosci.* **27** 3046 (2007)
86. Franks K M, Stevens C F, Sejnowski T J *J. Neurosci.* **23** 3186 (2003)
87. Nimchinsky E A et al. *J. Neurosci.* **24** 2054 (2004)
88. Paulsson J *Nature* **427** 415 (2004)
89. Lindner B et al. *Phys. Rep.* **392** 321 (2004)
90. Burkitt A N *Biol. Cybern.* **95** 97 (2006)
91. Ma J, Tang J *Sci. China Technol. Sci.* **58** 2038 (2015)
92. Lin H et al. *Nonlinear Dyn.* **106** 959 (2021)
93. Turrigiano G G et al. *Nature* **391** 892 (1998)
94. Niven J E et al. *Nature* **421** 630 (2003)
95. Bloss E B et al. *Nat. Neurosci.* **21** 353 (2018)
96. Zador A *J. Neurophysiol.* **79** 1219 (1998)
97. Manwani A, Koch C *Neural Comput.* **13** (1) 1 (2001)
98. Tarr T B, Dittrich M, Meriney S D *Trends Neurosci.* **36** (1) 14 (2013)
99. Maršálek P, Koch C, Maunsell J *Proc. Natl. Acad. Sci. USA* **94** 735 (1997)
100. Poliakov A V, Powers R K, Binder M D *J. Physiol.* **504** 401 (1997)
101. Deweese M R, Zador A M *J. Neurophysiol.* **92** 1840 (2004)
102. de Lafuente V, Romo R *Nat. Neurosci.* **8** 1698 (2005)
103. de Lafuente V, Romo R *Proc. Natl. Acad. Sci. USA* **103** 14266 (2006)
104. Pisarchik A N, Hramov A E *Multistability in Physical and Living Systems*: *Characterization and Applications* (Springer Series in Synergetics) (Cham: Springer, 2022) https://doi.org/10.1007/978-3-030-98396-3
105. Green D M, Swets J A *Signal Detection Theory and Psychophysics* Vol. 1 (New York: Wiley, 1966)
106. Deco G et al. *Proc. Natl. Acad. Sci. USA* **104** 20073 (2007)
107. Brunel N, Wang X-J *J. Comput. Neurosci.* **11** 63 (2001)
108. Deco G et al. *PLoS Comput. Biol.* **4** (8) e1000092 (2008) https://doi.org/10.1371/journal.pcbi.1000092
109. Smith P L, Ratcliff R *Trends Neurosci.* **27** (3) 161 (2004)
110. Roxin A, Ledberg A *PLoS Comput. Biol.* **4** (3) e1000046 (2008) https://doi.org/10.1371/journal.pcbi.1000046
111. Buzsáki G, Draguhn A *Science* **304** 1926 (2004)
112. Ouyang G et al. *NeuroImage* **205** 116304 (2020)
113. Gang H et al. *Phys. Rev. Lett.* **71** 807 (1993)

114. Benzi R, Sutera A, Vulpiani A *J. Phys. A* **14** L453 (1981)
115. Pikovsky A S, Kurths J *Phys. Rev. Lett.* **78** 775 (1997)
116. Pisarchik A N et al. *Sci. Rep.* **9** 18325 (2019)
117. Andreev A V et al. *Chaos Solitons Fractals* **106** 80 (2018)
118. Toral R, Mirasso C R, Gunton J D *Europhys. Lett.* **61** 162 (2003)
119. Wang Q et al. *Phys. Rev. E* **80** 026206 (2009)
120. Lacasta A M, Sagués F, Sancho J M *Phys. Rev. E* **66** 045105 (2002)
121. Simonotto E et al. *Phys. Rev. Lett.* **78** 1186 (1997)
122. Pisarchik A N, Hramov A E *Phys. Rep.* **1000** 1 (2023)
123. Pisarchik A N, Chholak P, Hramov A E *Chaos Solitons Fractals X* **1** 100005 (2019)
124. Huidobro N et al. *Neurosci. Lett.* **664** 51 (2018)
125. van der Groen O, Wenderoth N *J. Neurosci.* **36** 5289 (2016)
126. van der Groen O et al. *PLoS Comput. Biol.* **14** (7) e1006301 (2018) https://doi.org/10.1371/journal.pcbi.1006301
127. Mendez-Balbuena I et al. *J. Neurosci.* **32** 12612 (2012)
128. Ferrera V P, Rudolph K K, Maunsell J H *J. Neurosci.* **14** 6171 (1994)
129. Shadlen M N, Newsome W T *J. Neurophysiol.* **86** 1916 (2001)
130. Hebb D O *The Organization of Behavior*; *a Neuropsychological Theory* (New York: Wiley, 1949)
131. Köhler W, Wallach H *Proc. Am. Philos. Soc.* **88** 269 (1944)
132. Burns B D *The Uncertain Nervous System* (London: Edward Arnold, 1968)
133. Sterzer P, Kleinschmidt A, Rees G *Trends Cogn. Sci.* **13** (7) 310 (2009)
134. Carter O L, Pettigrew J D *Perception* **32** 295 (2003)
135. Moreno-Bote R, Rinzel J, Rubin N *J. Neurophysiol.* **98** 1125 (2007)
136. Pisarchik A N et al. *Biol. Cybern.* **108** 397 (2014)
137. Lago-Fernández L F, Deco G *Neurocomputing* **44–46** 503 (2002)
138. Laing C R, Chow C C *J. Comput. Neurosci.* **12** 39 (2002)
139. Wilson H R, Blake R, Lee S-H *Nature* **412** 907 (2001)
140. Huguet G, Rinzel J, Hupé J-M *J. Vision* **14** (3) 19 (2014)
141. Urakawa T, Bunya M, Araki O *Cogn. Neurodyn.* **11** 307 (2017)
142. Haken H *Synergetic Computers and Cognition*: *A Top-Down Approach to Neural Nets* (Berlin: Springer, 2004)
143. Jaimes-Reátegui R et al. *Discontinuity Nonlinearity Complex* **9** (1) 167 (2020)
144. Chholak P, Hramov A E, Pisarchik A N *Nonlinear Dyn.* **100** 3695 (2020)
145. Chholak P et al. *Front. Hum. Neurosci.* **14** 555 (2020)
146. Merk I, Schnakenberg J *Biol. Cyber.* **86** 111 (2002)
147. Meilikhov E Z, Farzetdinova R M *Cogn. Neurodyn.* **13** 613 (2019)
148. Maksimenko V A et al. *PloS ONE* **12** (12) e0188700 (2017)
149. Maksimenko V A et al. *Nonlinear Dyn.* **95** 1923 (2019)
150. Runnova A E et al. *Chaos Solitons Fractals* **93** 201 (2016)
151. Poston T, Stewart I *Catastrophe Theory and Its Applications* (London: Pitman, 1978)
152. Miller K J *J. Neurosci.* **30** 6477 (2010)
153. He B J *Trends Cogn. Sci.* **18** (9) 480 (2014)
154. Karpov O E et al. *Phys. Rev. E* **103** 022310 (2021)
155. Wilkat T, Rings T, Lehnertz K *Chaos* **29** 091104 (2019)
156. Boccaletti S, Pisarchik A N, del Genio C I, Amann A *Synchronization*: *from Coupled Systems to Complex Networks* (Cambridge: Cambridge Univ. Press, 2018)
157. Chholak P, Kurkin S A, Hramov A E, Pisarchik A N *Appl. Sci.* **11** 375 (2021)
158. Hramov A E, Maksimenko V A, Pisarchik A N *Phys. Rep.* **918** 1 (2021)
159. Hong S L, Rebec G V *Front. Aging Neurosci.* **4** 27 (2012)
160. Li S-C, Lindenberger U, Sikström S *Trends Cogn. Sci.* **5** (11) 479 (2001)
161. Serletis D et al. *Ann. Biomed. Eng.* **39** 1768 (2011)
162. Cremer R, Zeef E J *J. Gerontol.* **42** 515 (1987)
163. Davis G, Plaisted-Grant K *Autism* **19** 351 (2015)
164. Milne E *Front. Psychol.* **2** 51 (2011)
165. Belmonte M K et al. *Mol. Psychiatry* **9** 646 (2004)
166. Domínguez L G, Velázquez J L P, Galán R F *PLoS ONE* **8** (4) e61493 (2013)
167. Minshew N J, Williams D L *Arch. Neurol.* **64** 945 (2007)
168. Mohammad-Rezazadeh I et al. *Curr. Opin. Neurol.* **29** 137 (2016)
169. Sysoeva O. et al. *Sci. Rep.* **13** 12932 (2023)
170. Ebrahimi-Fakhari D, Sahin M *Curr. Opin. Neurol.* **28** 91 (2015)
171. Hramov A E et al. *Phys. Usp.* **64** 584 (2021); *Usp. Fiz. Nauk* **191** 614 (2021)
172. Smit D J A et al. *Human Brain Mapping* **29** 1368 (2008)
173. Iossifov I et al. *Nature* **515** 216 (2014)
174. Winterer G et al. *Clin. Neurophysiol.* **111** 837 (2000)
175. Schmitt N *Psychol. Assess.* **8** 350 (1996)
176. Winterer G et al. *Am. J. Psychiatry* **161** 490 (2004)
177. Kishore V, Santhanam M S, Amritkar R E *Phys. Rev. Lett.* **106** 188701 (2011)
178. Boers N et al. *Nat. Commun.* **5** 5199 (2014)
179. Albeverio S, Jentsch V, Kantz H (Eds) *Extreme Events in Nature and Society* (Berlin: Springer, 2006) https://doi.org/10.1007/3-540-28611-X
180. Osorio I et al. *Phys. Rev. E* **82** 021919 (2010)
181. Kuhlmann L et al. *Nat. Rev. Neurol.* **14** 618 (2018)
182. Frolov N, Hramov A *Chaos* **31** 063103 (2021)
183. Frolov N, Hramov A *Phys. Rev. E* **106** 044301 (2022)
184. Gloor P, Fariello R G *Trends Neurosci.* **11** (2) 63 (1988)
185. Frolov N S et al. *Sci. Rep.* **9** 7243 (2019)
186. Pisarchik A N et al. *Eur. Phys. J. Spec. Top.* **227** 921 (2018)
187. Bak P, Tang C, Wiesenfeld K *Phys. Rev. Lett.* **59** 381 (1987)
188. Corbalán R et al. *Phys. Rev. A* **51** 663 (1995)
189. Huerta-Cuellar G et al. *Phys. Rev. E* **79** 036204 (2009)
190. Pisarchik A N, Pochepen O N, Pisarchyk L A *PLoS ONE* **7** e46582 (2012)
191. Stolbova V et al. *Geophys. Res. Lett.* **43** 3982 (2016)
192. Bakdash J Z, Marusich L R *Front. Psychol.* **8** 456 (2017)
193. Scheffer M et al. *Nature* **461** 53 (2009)
194. Meisel C, Kuehn C *PLoS ONE* **7** e30371 (2012) https://doi.org/10.1371/journal.pone.0030371
195. Chang W-C et al. *Nat. Neurosci.* **21** 1742 (2018)
196. Maturana M I et al. *Nat. Commun.* **11** 2172 (2020)
197. Maksimenko V A et al. *Sci. Rep.* **7** 2487 (2017)
198. Pisarchik A N, Maksimenko V A, Hramov A E *J. Med. Internet Res.* **21** e16356 (2019)
199. Cortes-Briones J A et al. *Biol. Psychiatry* **78** 805 (2015)
200. D'Souza D C et al. *Neuropsychopharmacology* **37** 1632 (2012)
201. Lempel A, Ziv J *IEEE Trans. Inform. Theory* **22** 75 (1976)
202. Friedman D, Simpson G, Hamberger M *Psychophysiology* **30** 383 (1993)
203. Rossini P M, Rossi S *Neurology* **68** 484 (2007)
204. Allen P A, Coyne A C *Exp. Aging Res.* **14** (3) 143 (1988)
205. Allen P A, Coyne A C *Exp. Aging Res.* **14** (3) 151 (1988)
206. Allen P A *Cogn. Dev.* **5** 177 (1990)
207. Myerson J et al. *Psychol. Rev.* **97** 475 (1990)
208. Allen P A, Madden D J, Crozier L C *Psychol. Aging* **6** 261 (1991)
209. Allen P A et al. *J. Gerontol.* **47** (2) P69 (1992)
210. Allen P A et al. *J. Gerontol.* **47** (5) P344 (1992)
211. Reuter-Lorenz P, Sylvester C, in *Cognitive Neuroscience of Aging*: *Linking Cognitive and Cerebral Aging* (Eds R Cabeza, L Nyberg, D Park) (Oxford: Oxford Univ. Press, 2005) p. 186
212. Fjell A M, Walhovd K B *Rev. Neurosci.* **21** (3) 187 (2010)
213. Raz N et al. *Cerebral Cortex* **15** 1676 (2005)
214. Crossman E R, Szafran J *Experientia* (Suppl. 4) 128 (1956)
215. Voytek B et al. *J. Neurosci.* **35** 13257 (2015)
216. Podvalny E et al. *J. Neurophysiol.* **114** 505 (2015)
217. Dave S, Brothers T A, Swaab T Y *Brain Res.* **1691** 34 (2018)
218. Lalwani P, Garrett D D, Polk T A *J. Neurosci.* **41** 9350 (2021)
219. Li S-C et al. *Neurosci. Biobehav. Rev.* **30** 775 (2006)
220. Li S C, von Oertzen T, Lindenberger U *Neurocomputing* **69** 1553 (2006)
221. Attwell D, Laughlin S B *J. Cereb. Blood Flow Metab.* **21** 1133 (2001)
222. Balasubramanian V, Kimber D, Berry M J (II) *Neural Comput.* **13** 799 (2001)
223. De Polavieja G G *J. Theor. Biol.* **214** 657 (2002)
224. Yu L, Yu Y *J. Neurosci. Res.* **95** 2253 (2017)